Luís Carlos Serrachino Granadeiro

"Effects of vitamin K deficiency and its mechanisms in vertebrate's early development: zebrafish as a model."

Universidade do Algarve

Departamento de Ciências Biomédicas e Medicina

2015

Luís Carlos Serrachino Granadeiro

"Effects of vitamin K deficiency and its mechanisms in vertebrate's early development: zebrafish as a model."

Mestrado em Ciências Biomédicas
Master's Degree in Biomedical Sciences

Supervisors:

Dr. Ignacio Fernández

Dr. Paulo J. Gavaia

Universidade do Algarve

Departamento de Ciências Biomédicas e Medicina

2015

Declaro ser o autor deste trabalho, que é original e inédito. Autores e trabalhos consultados estão devidamente citados no texto e constam da listagem de referências incluída.

I declare to be the author of this work, which is original and unpublished. Authors and studies reviewed are properly cited in the text and contained in the included references list.

_____

(Luís Carlos Serrachino Granadeiro)

Agradecimentos /Acknowledgements

Em primeiro lugar gostaria de agradecer à professora Dra. Maria Leonor Cancela por me ter disponibilizado o seu laboratório, sem o qual nada poderia ter sido feito. Agradecer também a todos os elementos que fizeram ou fazem parte da equipa do Bioskel, que de alguma forma ajudaram para que este trabalho se concretizasse. Agradeço também ao Dr. Paulo Gavaia, por toda a orientação prestada durante a realização deste relatório, e por todo o apoio.

De uma forma mais especial, quero agradecer ao Dr. Ignacio Fernández, por tudo o que fez por mim, por toda a paciência, disponibilidade e conhecimentos prestados, essenciais para que esta tese progredisse com sucesso, mas em especial pelo amigo que foi durante todo este tempo. Muito obrigado Nacho!

Abstract

Vitamin K (VK) acts as a cofactor of the enzyme γ-glutamyl carboxylase (Ggcx) promoting the γ-carboxylation of VK dependent proteins (VKDP), where a posttranslational conversion of Glu into Gla residues is achieved, providing calcium binding properties to VKDPs. Some VKDPs are involved in blood clotting but also in other processes. During γ-carboxylation, the reduced VK is converted to the epoxide form, which is then recycled back into VK by the enzyme VK epoxide reductase (Vkor).

Warfarin inhibits Vkor activity, being used to control blood clotting through the reduction of the γ-carboxylation of coagulation factors in patients who are at risk of venous thromboembolism. However, it might affect the activity of other VKDP. When administered during pregnancy, it induces fetal morbidity and mortality in pregnant women, being this associated with bleeding disorders and skeletal deformities. In this work the effects of VK deficiency in vertebrate's early development were evaluated using zebrafish (*Danio rerio*) as a model. Zebrafish (embryos and larvae) were exposed to increasing levels of warfarin (0, 5, 25 and 125 mg L^{-1}) during two critical periods: 0-2.5 (embryonic development) and 2.5-5 (endotrophic larvae) days post fertilization. Larvae exposed to high concentrations of warfarin showed growth retardation, bleeding, underdeveloped swimbladder, pericardial inflammation, disruption of skeletogenesis, and increased mortality. The effects were much more severe when they were exposed to the anticoagulant during the embryonic stage. Regarding skeletogenesis, mineralization of several cranial structures as well as the axial skeleton was reduced. The length of the endochodral structures in the cranial region was also shorter in warfarin exposed larvae. Expression of genes involved in skeletogenesis (*sox9*, *runx2*, *osx*, *col2a1*, *grp1*, *alp*, *mgp* and *bgp*) was affected depending on the developmental stage analyzed. Present work brings new insights on the particular mechanisms by which warfarin (and thus, VK deficiency) affects chondrogenesis and osteoblastogenesis.

Key-words: Vitamin K; warfarin; zebrafish; skeletogenesis; Warfarin Embryopathy; gene expression.

Resumo

A vitamina K (VK) é uma vitamina lipossolúvel que atua como cofator da enzima γ-glutamil carboxilase (Gccx) de forma a promover a γ-carboxilação das proteínas dependentes de VK (VKDP). Neste processo ocorre uma modificação pós-tradução que é responsável por converter os resíduos de glutamato (Glu) que estão presentes nas VKDP em resíduos γ-carboxilglutamato (Gla), que são necessários para promover a sua ligação a iões de cálcio de maneira a que estas possam desempenhar corretamente as suas funções. As VKDPs estão envolvidas na coagulação do sangue (fatores de coagulação), mas também em outros processos, entre os quais a esqueletogénese. Durante a γ-carboxilação, a forma reduzida da VK é convertida para a forma de epóxido, que é depois reciclada de volta para VK pela enzima VK epóxido redutase (Vkor), de maneira que esta possa ser novamente usada. A forma reduzida da VK tem uma elevada capacidade antioxidante e pode ligar-se ao recetor X de pregnano (Pxr). Através desta ligação a VK também tem um papel na transcrição, uma vez que o Pxr controla a transcrição de vários genes envolvidos tanto no processo de desintoxicação do organismo como na homeostasia óssea.

A Varfarina, um derivado de cumarina com baixo peso molecular é um inibidor da atividade da Vkor. Neste sentido, uma vez que a varfarina bloqueia a reciclagem de VK, esta é usada para controlar a coagulação do sangue através da redução da γ-carboxilação dos fatores de coagulação (e portanto a sua atividade) em pacientes que estão em risco de tromboembolismo venoso. A varfarina está associada a diversos problemas em humanos, como calcificação vascular devido à inibição da γ-carboxilação de diversas VKDP não relacionadas com a coagulação sanguínea, tais como a proteína Gla óssea (Bgp), a proteína Gla da matriz (Mgp) e a proteína rica em Gla (Grp). Vários outros anticoagulantes foram desenvolvidos e estão a ser testados clinicamente, contudo problemas associados a estes têm surgido, como é o caso do aumento do risco de infarto do miocárdio. Além disso, estes anticoagulantes não apresentam antidoto, sendo impossível reverter o seu efeito. Assim, embora a varfarina também afete a atividade de outras VKDP, continua a ser o anticoagulante mais eficaz e mais utilizado em todo o mundo. Quando administrada durante a gravidez, a varfarina tem a capacidade de atravessar a placenta induzindo morbilidade e mortalidade fetal em mulheres grávidas. A mortalidade fetal após exposição a varfarina é associada a eventos hemorrágicos e deformações esqueléticas

(*chondrodysplasia punctata*, dismorfismo facial com hipoplasia nasal, membros curtos entre outros), sendo esta condição patológica conhecida como embriopatia da varfarina.

Ao longo dos anos vários trabalhos têm demonstrado que a VK tem um papel importante no metabolismo do osso. Vários estudos em humano reportaram um efeito positivo da VK no osso, inibindo a diminuição da densidade mineral óssea e aumentando a resistência do mesmo. Além disso, trabalhos *in vitro* demonstraram que a VK está envolvida na promoção do crescimento e maturação osteoblástica (transição osteoblasto-osteócito) promovendo desta forma a mineralização, mediada em parte através da γ-carboxilação de VKDP. A VK está também envolvida na diminuição da reabsorção óssea (inibição da osteoclastogénese). Através da sua ligação ao recetor nuclear PXR regula também a homeostasia óssea, promovendo o aumento expressão de marcadores ósseos. Trabalhos *in vivo* também reforçam o papel da VK na esqueletogénese. Estudos verificaram que a suplementação de VK na dieta de larvas de linguado estava envolvida na modelação de proteínas envolvidas em vários processos biológicos, entre os quais o desenvolvimento ósseo, promovendo uma melhoria na qualidade da formação do osso. O efeito contrário foi também demonstrado; a deficiência em VK está na origem de distúrbios no desenvolvimento do peixe-zebra, sendo que também a esqueletogénese é afetada (aumento do número de deformações).

Neste trabalho propomo-nos a avaliar os efeitos promovidos pela deficiência em VK no desenvolvimento inicial de vertebrados utilizando o peixe-zebra (*Danio rerio*) como modelo. O peixe-zebra é um pequeno teleósteo de água doce que tem como principais características que o tornam um bom modelo de estudo a fecundação externa, a claridade ótica durante a embriogénese, o desenvolvimento rápido e a alta taxa de reprodução. Embriões e larvas de peixe-zebra foram expostos a níveis crescentes de varfarina (0, 5, 25 e 125 mg L^{-1}) durante dois períodos críticos do seu desenvolvimento: 0-2,5 (desenvolvimento embrionário) e 2,5-5 (desenvolvimento endotrófico) dias após a fertilização (dpf). Neste sentido, as larvas expostas a elevadas concentrações de varfarina (em particular a 125 mg L^{-1}) mostraram um atraso significativo no crescimento, eventos hemorrágicos, bexiga natatória subdesenvolvida, inflamação pericárdica, reabsorção do saco vitelino afetada e perturbação na esqueletogénese (mineralização e comprimento ósseo), levando a um aumento significativo da mortalidade. Os efeitos encontrados foram muito mais graves quando o peixe-zebra foi exposto ao anticoagulante durante a fase embrionária, sendo que estas larvas mostraram imitar a embriopatia da varfarina em

humanos. Quanto à esqueletogénese, verificou-se que a mineralização de várias estruturas cranianas (tais como o basioccipital, o opérculo, o cleitro, os arcos ceratohiais e o parasphenoide), bem como o esqueleto axial se encontrava reduzida. O comprimento das estruturas endocondrais na região craniana (cartilagem de Meckel, arcos ceratohiais, o primeiro arco ceratobranquial e a placa etmoide) também foi encontrado reduzido em larvas expostas a varfarina. A expressão de genes envolvidos na esqueletogénese (*sox9*, *runx2*, *osx*, *col2a1*, *grp1*, *alp*, *mgp* e *bgp*) foi também encontrada afetada, sendo que a alteração na expressão dependeu do estágio de desenvolvimento em que a análise foi feita. Enquanto aos 3 dpf as larvas expostas à varfarina mostraram uma alteração na expressão (subexpressão) em genes envolvidos na condrogénese (*sox9*, *col2a1* e *grp1*), aos 5 dpf a expressão de genes envolvidos na osteoblastogénese (*osx* e *alp*) foi encontrada alterada (subexpressão). Surpreendentemente, alguns genes envolvidos tanto na condrogénese como na osteoblastogénese (*runx2* e *osx*) foram encontrados sobre-expressos aos 16 dpf nas larvas expostas à varfarina, indicando um desenvolvimento tardio do esqueleto.

Neste sentido, o presente estudo traz novas visões em particular sobre os mecanismos pelos quais a varfarina (e portanto, a deficiência em VK) afeta tanto a condrogénese como a osteoblastogénese. Este estudo reforça também o importante papel que a VK tem no desenvolvimento inicial dos vertebrados.

Palavras-chave: vitamina K; varfarina; peixe-zebra; esqueletogénese; Embriopatia da varfarina; expressão génica.

Index

List of figures

List of tables

Abbreviations

3-KDS - 3-ketodihydrosphingosine

Alp - Alkaline phosphatase

Bgp - Bone gla protein

Bgp1 - Bone Gla Protein 1

Bgp2 - Bone Gla Protein 2

Bop - Basioccipital

Bp - Base pairs

Cbfa1 - Core-binding factor alpha 1

CCD - Cleidocranial dysplasia

CD - Campomelic dysplasia

cDNA - Complementary DNA

CO_2 - Carbon dioxide

Col2a1 - Collagen type 2 alpha 1

Col9a2 - Collagen type 9 alpha 2

Col11a2 - Collagen type 11 alpha 2

DEPC - Diethylpyrocarbonate

DNA - Deoxyribonucleic acid

DNase - Deoxyribonuclease

dNTP - Nucleotide triphosphates containing deoxyribose

Dpf - Days post fertilization

ECM - Extracellular matrix

EDTA - Ethylenediamine tetraacetic acid

EtBr - Ethidium bromide

EtOH - Ethanol

FWS - Fetal warfarin syndrome

GAGs - Glycosaminoglycans

Gas6 - Growth-arrest specific 6

Ggcx - Γ-glutamyl carboxylase

Gla - Γ-carboxyl glutamate

Glu - Glutamate

Grp - Gla-rich protein

Grp1 - Gla-rich protein 1

Grp2 - Gla-rich protein 2

HCl - Hydrochloric acid

H_2O – Water

H_2O_2 - Hydrogen peroxide

KOH - Potassium hydroxide

LB - Lysogeny broth

Mgp - Matrix gla protein

MK - Menaquinone

MK-4 - Menaquinone-4

M-MLV - Moloney-murine leukemia virus

mRNA - Messenger RNA

NaOH - Sodium hydroxide

NF-kB - Nuclear factor kappa-B

NR - Nuclear receptor

O_2 - Oxygen

ON - Overnight

OSE2 - Osteoblast-specific *cis*-acting element 2

Osx - Osterix

PBS - Phosphate Buffered Saline

PCR - Polymerase chain reaction

PFA - Paraformaldehyde

Pxr - Pregnane X receptor

RANK - Receptor activator of nuclear factor kβ

RANKL - Receptor activator of nuclear factor kβ ligand

RNA - Ribonucleic acid

RNAse - Ribonuclease

RT - Room temperature

RT-qPCR - real-time quantitative polymerase chain reaction

Runx1 - Runt-related transcription factor 1

Runx2 - Runt-related transcription factor 2

Runx3 - Runt-related transcription factor 3

Rxr - Retinoid X receptor

SDS - Sodium dodecyl sulfate

SOC - Super Optimal Broth with Catabolite repression

Sox9 - Sex determining region Y-box 9

Sxr - Steroid and xenobiotic receptor

Sxre - Steroid and Xenobiotic Receptor responsive elements

TRAP - Tartrate-resistant acid phosphatase

TF - Transcription factor

Tnap - Tissue-nonspecific alkaline phosphatase

UV - Ultraviolet light

VK - Vitamin K

VK_1 - Vitamin K 1

VK_2 - Vitamin K 2

VK_3 - Vitamin K 3

VKA - Vitamin K antagonist

VKDB - Vitamin K Deficiency Bleeding

VKDP - Vitamin K dependent protein

VKH_2 - Vitamin K hydroquinone

Vkor - Vitamin K epoxide reductase

Vkorc1 - Vitamin K epoxide reductase complex subunit 1

Vkorc1l1 - vitamin K epoxide reductase complex subunit 1-like protein 1

VKR - Vitamin K reduction

WE - Warfarin Embryopathy

X-Gal - 5-bromo-4-chloro-3-indolyl-β-D-galactopyranoside

Chapter 1
Introduction

1. Introduction

1.1 Skeleton: functions, tissues and cell types

The skeleton, formed mainly by bone and cartilage, plays important functions in the organism providing internal support and protection to vital organs. Further, together with the musculature it allows the locomotion. In mammals, bone is also a source of calcium and phosphate under specific conditions and holds the house of the hematopoietic system (reviewed in Hall, 2015).

Cartilage, unlike bone, is an avascularized and anaerobic tissue consisting of cells in an extracellular matrix (ECM; reviewed in Hall, 2015). Cartilage cells are generally the chondroblasts and the chondrocytes (cartilage forming and homeostasis), which are derived from mesenchymal stem cells, being responsible to secrete a cartilaginous ECM (Myllyharju, 2014). ECM in cartilage is composed by specific types of collagens, glycosaminoglycans (GAGs), proteoglycans and water. The major collagen is the type II, however other collagen types, such as VI, IX and XI are present. In particular hypertrophic chondrocytes are characterized by the production of type 10 collagen. Regarding to proteoglycans, aggrecan is the major component (Myllyharju, 2014).

Bone is an aerobic and vascularized tissue consisting of cells and an ECM. The main bone cell types are the osteoblasts (bone-forming cells), the osteocytes (bone homeostasis), and the osteoclasts (bone remodeling). Osteoblasts are cells derived from mesenchymal stem cells and are responsible for synthetizing the ECM. When they become trapped into ithe ECM, they are called osteocytes (Franz-Odendaal et al., 2006). Osteocytes are osteoblast-derived cells involved in bone homeostasis, regulating some bone responses to particular stimulus, such as damages and mechanical loads. Osteocytes can communicate with neighboring osteocytes and with the other cells on the bone surface via canaliculi within the bone matrix. Through this communication, osteocytes are involved in the regulation of the deposition of bone matrix, modulation of osteoclast activity, but also in the resorption of the perilacunar bone (osteocytic osteolisys; reviewed in Hall, 2015). They are by far the most abundant cellular component of bones, making up 95% of all bone cells (Franz-Odendaal et al., 2006). Interestingly, bone can be classified by the presence or absence of osteocytes in the ECM, so in this sense, bone may be cellular (osteocytic) or acellular (anosteocytic; reviewed in Hall, 2015). Finally, osteoclasts are

mono or multinucleated cells of hematopoietic origin responsible for bone remodeling (Witten et al., 2001; Boyle et al., 2003). The mature osteoclasts are activated by external signals like the activation of receptor activator of nuclear factor kβ (RANK) by its ligand RANKL inducing internal structural changes to prepare them for bone resorption. In this sense, rearrangements of the actin cytoskeleton and formation of a tight junction between the bone surface and basal membrane form a sealed compartment which is then acidified by the export of hydrogen ions (Boyle et al., 2003). Secretion continues with the export of the lytic enzymes Tartrate-resistant acid phosphatase (TRAP) and pro-cathepsin K into a resorption pit called as Howship's lacunae (Boyle et al., 2003). In contrast to cartilage ECM, bone ECM is composed essentially by inorganic components (65%-70% of total ECM) such as calcium and phosphate but also by organic components (35%-30% of total ECM) such as collagen fibers (mainly type I collagen) and other non-collagenous proteins such as proteoglycans, growth factors, and other bone matrix proteins, such as bone Gla protein (Bgp), osteopontin, osteonectin and matrix Gla protein (Mgp; reviewed in Jiang et al., 2007; Hall, 2015). The first bone matrix is formed in an unmineralized state, known as osteoid, being then impregnated with hydroxyapatite to form bone (Hall, 2015).

1.2 Bone formation and mineralization

Bone can form through two different processes. In one hand, most of the mammalian skeleton is formed by endochondral ossification, which involves a cartilage intermediate.

In this process mesenchymal stem cells form condensations and differentiate into chondroblasts (Fig. 1.1A; Crombrugghe et al., 2001). Bone growth occurs through a specialized cartilaginous structure, named growth plate, where an ordered zone of proliferating and differentiating chondrocytes produce the extracellular matrix (Fig. 1.1B; Myllyharju, 2014). These chondrocytes undergoing unidirectional proliferation become hypertrophic and start to mineralize the ECM before entering in apoptosis (Fig. 1.1C; Crombrugghe et al., 2001). At the same time that chondrocyte hypertrophy occurs, some of the mesenchymal stem cells surrounding cartilage start to differentiate leading to the appearance of osteoblasts (Fig. 1.1D). These osteoblasts invade the zones of hypertrophic chondrocytes together with blood vessels and osteoclasts (Fig. 1.1E). While osteoclasts degrade the hypertrophic cartilage matrix, osteoblasts use the remnants of cartilage matrix as a scaffold for the deposition of bone matrix (Crombrugghe et al., 2001).

On the other hand, a small number of skeletal elements, mainly craniofacial and flat bones, are formed by intramembranous ossification. Here, bones form through mesenchymal stem cell condensations that differentiate directly into osteoblasts, without a cartilage template (Crombrugghe et al., 2001).

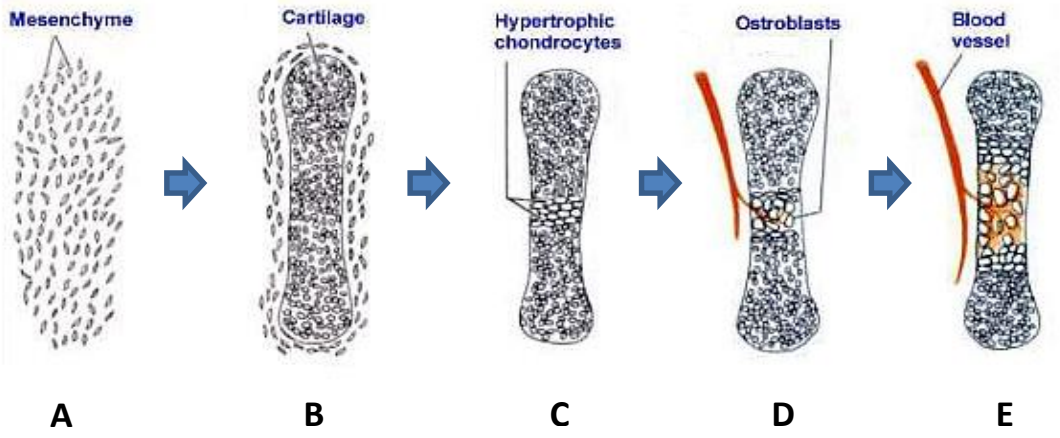

Figure 1.1. General illustration of the endochondral ossification process. Cells in the condensations differentiate into chondrocytes (A-B). These chondrocytes undergo unidirectional proliferation, becoming hypertrophic (C). At the same time that chondrocyte hypertrophy occurs, some of the mesenchymal cells surrounding cartilage start to differentiate into osteoblasts (D). These osteoblasts invade the zones of hypertrophic chondrocytes together with blood vessels and osteoclasts (E). Figure adapted from http://www.anatomiahumana.ucv.cl/kine1/top2.html.

1.3 Transcriptional control of bone formation and homeostasis

Early development of the skeleton is dependent on factors which have crucial roles in the cell-fate process by which mesenchymal cells become chondrocytes and osteoblasts (Fig. 1.2; reviewed in Sinha and Zhou, 2013). These are transcription factors (TF) and nuclear receptors (NR). TFs are proteins that can bind to specific DNA sequences, thereby controlling the rate of transcription of genetic information from DNA by promoting or blocking the transcription of specific genes (Latchman, 1997; Lee and Young, 2000). NRs are transcription factors that respond to signals carried by steroids, thyroid hormones and other molecules such as vitamins. Through this interaction they are able to regulate the expression of specific genes by its binding to specific DNA sequences (reviewed in Huang et al., 2010). Some TFs important in bone formation will be described (Runx2, Sox9 and Osterix) as well as NRs such as the pregnane X receptor (Pxr), a nuclear receptor involved in bone homeostasis (Azuma et al., 2010).

Sex determining region Y-box 9 (Sox9) is a member of the TFs Sox family, being required for testogenesis, chondrogenesis, terminal differentiation of oligodendrocytes and cardiogenesis (Mori-Akiyama et al., 2003 Akiyama, 2008). Regarding its role in chondrogenesis, Sox9 is crucial for the commitment of osteochondroprogenitors, chondrogenic mesenchymal condensation and proper chondrocyte proliferation, differentiation, maturation and hypertrophic conversion (Akiyama, 2008). During embryogenesis it is expressed in all chondroprogenitors and chondrocytes, except in the hypertrophic (Akiyama, 2008). Studies have showed that Sox9-null cells do not express chondrogenic marker genes, such as *col2a1*, *col9a2*, *col11a2*, and *aggrecan* (Akiyama, 2008). Further, mutations in one allele of *Sox9* in humans result in campomelic dysplasia (CD), a skeletal dysplasia characterized by sex reversal and skeletal malformations of endochondral bones (Mori-Akiyama et al., 2003; Akiyama, 2008).

The runt-related TFs family includes Runx1, Runx2 and Runx3. These factors are essential for hematopoietic (Runx1), neuronal, gastrointestinal (Runx3) and osteochondrogenic (Runx2) differentiation (reviewed in Ziros et al., 2008). In particular Runx2, also known as core-binding factor alpha 1 (Cbfa1) is essential in the terminal differentiation of chondrocytes, a prerequisite for endochondral ossification. During osteoblast differentiation, Runx2 play essential roles in the commitment of pluripotent mesenchymal cells to the osteoblastic lineage (reviewed in Komori, 2010). There are two known isoforms of Runx2. The type I seems to be mainly involved in intramembranous bone formation (reviewed in Ziros et al., 2008). The type II isoform is exclusively involved in endochondral bone formation. Runx2 operates by binding to osteoblast-specific *cis*-acting element 2 (OSE2), which is found in the promoter region of all major osteoblast-related genes (reviewed in Ziros et al., 2008). Studies have demonstrated that mice with a mutated *runx2* locus have a complete lack of ossification due to the maturational arrest of osteoblasts (reviewed in Ziros et al., 2008).

Like Runx2, Osterix (Osx; also known as Sp7 TF) is a major and essential effector for osteoblast differentiation, activating bone-specific genes that support bone formation (reviewed in Shina and Zhou, 2013). Mice lacking Osx die within 1 h of birth with a complete absence of intramembranous and endochondral bone formation (Baek et al., 2009).

Pxr (also known as steroid and xenobiotic receptor; SXR) is a member of the NR superfamily NR1I, it is mainly expressed in the liver and intestine where it acts as a

xenobiotic sensor. In fact, it plays important roles on different processes like the detoxification of the organism (drug metabolism), bone homeostasis, but also regulating metabolic pathways for the elimination of cholesterol and regulating the glucose metabolism (Timsit and Negishi, 2007). Pxr can be activated by various endogenous and dietary substances such as vitamin K (VK), pharmaceutical agents and xenobiotic compounds (Ekins et al., 2008). Recently, Wallace et al. (2013) described the 3D structure the heterodimer formed by Pxr and the retinoid X receptor (Rxr). The formed complex will bind to Sxr responsive elements (Sxre) in the promotor or enhancer regions of target genes, activating their transcription. Although expression of *pxr* was detected at lower levels in bone, being found in osteoblasts (Tabb et al., 2003; Azuma et al., 2010); Azuma and colleagues (2010) have demonstrated that systemic Pxr deficiency results in osteopenia. They also saw through histomorphometrical analysis of trabecular bones that bone formation parameters (bone mineral density and stiffness) were decreased in *pxr* knock-out compared with WT mice, suggesting Pxr loss-of-function result in suppressed osteoblastic function (Azuma et al., 2010). Pxr also affected calcium and phosphate homeostasis through the induction of vitamin D-catabolizing enzyme CYP3A4 in the liver and intestine (Zhou et al., 2006). VK_2, according to Tabb et al. (2003), can have important roles in bone development by binding to Pxr, through the regulation of the transcription of bone markers such as *alp*, *mgp* and *opn*. Further characterization of how VK2 induce osteoblast function through Pxr at transcriptional level of other osteoblastic genes (*tsukushi*, *matrilin-2* and *CD14 antigen*) was reported by Ichikawa et al. (2006). In addition, other possible pathways by which Pxr affect bone metabolism can be the suppression of the nuclear factor kappa-B (NF-kB) signalling (Gu et al., 2006). NF-kB was reported as a promoter of osteoclastogenesis (Jimi et al., 2004) and inhibitor of bone formation by mature osteoblast (Chang et al., 2009).

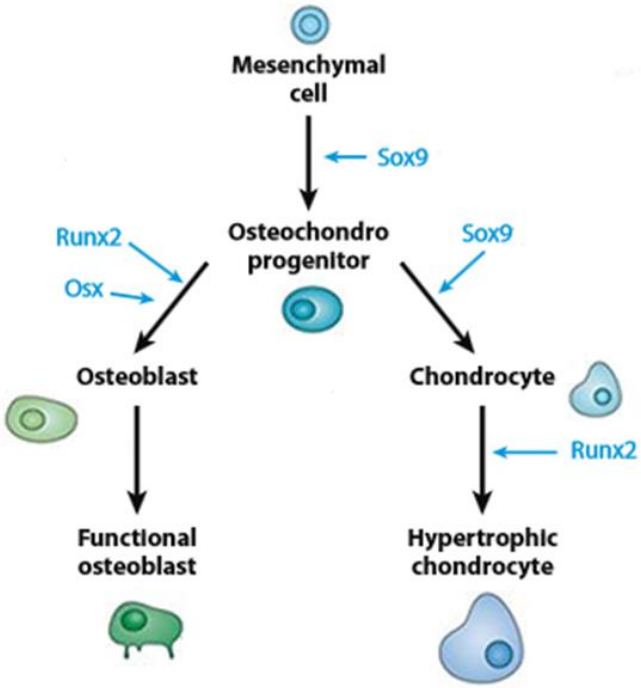

Figure 1.2. Transcriptional roles of Sox9, Runx2 and Osx in the cell-fate process by which mesenchymal cells become chondrocytes and osteoblasts. Sox9 is crucial for the commitment of osteochondroprogenitors, chondrogenic mesenchymal condensation and proper chondrocyte proliferation, differentiation, maturation and hypertrophic conversion. Runx2 is essential for chondrocyte and osteoblast differentiation. Osx, together with Runx2, is essential for osteoblast differentiation and function. Figure modified from Karsenty, 2008.

1.4 Vitamin K

Vitamin K (VK) belongs to the group of fat-soluble vitamins, being only *de novo* synthesized by plants and bacteria. There are two natural metabolites, phylloquinone (VK_1) and menaquinone (VK_2), and a synthetic one, menadione (VK_3; Oldenburg et al., 2008). VK_1 is synthesized by plants while VK_2 or menaquinones (MK) are synthesized by a limited number of obligate and facultative anaerobic bacteria, some of which occupy the microflora of the human gut (reviewed in Shearer and Newman, 2014). The MK family contains a wide spectrum of isoprenologs being named according to the number of these prenyl units (MK-n; reviewed in Shearer and Newman, 2014). VK is predominantly present in the forms of VK_1 and menaquinone-4 (MK-4), which is now known to be synthesized in human from VK_1 by the UbiA prenyltransferase containing 1 (Ubiad1) enzyme (Ferland, 2012).

VK in lower organisms has an important role as electron carrier in energy transduction pathways (Oldenburg et al., 2008). In contrast, in higher organisms, the VK family members have been studied during decades due to its important role on blood coagulation process (Oldenburg et al., 2008). In this sense VK acts as cofactor of the γ-glutamyl carboxylase (Ggcx) enzyme, which is responsible to perform posttranslational γ-carboxylation of vitamin K dependent proteins (VKDPs). VK (reduced form VKH_2) was also recognized as having a potent antioxidant capacity (Mukai et al., 1993; Fig. 1.3).Also Li et al. (2003) had demonstrated that cell death caused by oxidative stress can be prevented in cultures of neuronal cells by VK_1 and VK_2 through the blockage of reactive oxygen species (ROS) accumulation. More recently, Westhofen et al. (2011) suggested that one of the enzymes responsible for VK recycling, Vitamin K epoxide reductase complex subunit 1-like protein 1 (Vkorc1l1), is responsible for VK-mediated increased survival of cells under oxidative stress limiting the amount of intracellular ROS in vitro. In addition, VK was identified as a specific ligand of Pxr (Tabb et al., 2003; Fig. 1.3). In this sense therefore, VK also have a transcriptional role, controlling different pathways through its binding to this nuclear receptor (Tabb et al., 2003).

Beside the roles above described, VK is also important in sphingolipid metabolism. VK promotes the induction of 3-ketodihydrosphingosine synthase (3-KDS), the enzyme involved in the initial step of sphingolipid biosynthesis (reviewed in Ferland, 2012). Sphingolipids are a group of complex lipids present in cells, being the major components of cell membranes (reviewed in Ferland, 2012), and are viewed as crucial players of important cellular events such as proliferation, differentiation, senescence and cell–cell interaction (reviewed in Ferland, 2012).

1.5 Vitamin K cycle

In mammals, recycling of VK (Fig. 1.3) is extremely important, since VK reservoirs in the organism are low. As described before, VK plays important roles, such as acting as a cofactor to the Ggcx enzyme, which is responsible for the posttranslational modification of glutamate (Glu) to γ-carboxylglutamate (Gla) required for the activity of VKDPs, conferring them calcium binding properties (reviewed in Stafford, 2005; Oldenburg et al., 2008). The γ-carboxylation reaction requires the propeptide-containing substrate and three co-substrates: reduced VK (reduced form, VKH_2), CO_2 and O_2. The rate of γ-carboxylation

is mainly controlled by the level of VKH_2 available for the reactions; while the dissociation rate constant is dependent upon both the propeptide and the Gla domain of the substrate. To promote the γ-carboxylation the subtraction of a proton from the carbon 4 of glutamate by VKH_2 is required, and results in the conversion of VKH_2 to VK epoxide. The epoxide form must be recycled to VK before it can be reused, a reaction catalyzed by the enzyme vitamin K epoxide reductase (Vkor; reviewed in Stafford, 2005). In contrast to genomes of archaea, eubacteria, plants, protists, and lower animals that include a single Vkor protein, the vertebrate genomes include two paralogous enzymes, Vitamin K epoxide reductase complex subunit 1 (Vkorc1) and Vitamin K epoxide reductase complex subunit 1-like protein 1 (Vkorc1l1; Westhofen et al., 2011). Westhofen et al., (2011) suggested that both enzymes have different functions; Vkorc1 is responsible for converting the epoxide in VK, being then Vkorc1-like 1 responsible for reducing the VK to its active form (VKH_2; Westhofen et al., 2011). That author suggests that Vkorc1 is more efficient at de-epoxidation (Vkor activity), whereas Vkorc1l1 is more efficient at converting quinone to hydroquinone reduction (VKR activity; Westhofen et al., 2011). However, Hammed et al. (2013) showed recently that Vkorc1l1 is also able to support Vkor activity and can be an alternative pathway able to substitute or partially complement for loss of Vkorc1 function in various non-hepatic tissues of vkorc1 knockout mice. Thus, it seems that both enzymes are able to support Vkor and VKR activity, being responsible for *de novo* reduction of VK in the VK cycle (Oldenburg et al., 2015).

Although VK recycling is crucial to restore the levels of this vitamin available in organisms, it can be blocked by some anticoagulants (coumarins), which are specific inhibitors of Vkor activity and called as vitamin K antagonists (VKA; Fig. 1.3). Anticoagulant therapy is particularly recommended to prevent and treat thromboembolic conditions in patients who have prosthetic heart valves but also with history/symptoms of excessive levels of blood coagulation (How, 2004; Moyer et al., 2009). Commonly are used those comprising parenteral anticoagulants, such as unfractionated heparin, low-molecular-weight heparin or fondaparinux, but also VKA such as warfarin, acenocumarol or phenprocoumon (coumarin derivatives; Beinema et al., 2008; Gómez-Outes et al., 2009). Other anticoagulants have been recently developed, such as dabigatran, rivaroxaban, apixaban, edoxaban or betrixaban (Gómez-Outes et al., 2013). However, this new molecules are more problematic anticoagulant therapies, since in general they (specifically targeting Thrombin and FXa) have no antidote (Gómez-Outes et al., 2013). In

addition, other particularities have been described, such as an increase of myocardial infarction risk when patients are under Dabigatran therapy (Kohli and Cannon, 2013).

Nowadays, the most used anticoagulant is warfarin (3-(a-acetonylbenzyl)-4-hydroxycoumarin). Warfarin is a low molecular weight drug derived from coumarins being a racemic mixture of R and S enantiomers, with the S enantiomer being about three times more potent than the R enantiomer (Kamali and Wynne, 2010). Since it acts as VKA, this effect is used in oral anticoagulation treatments for thromboembolic disorders, controlling the γ-carboxylation of coagulation factors (Oldenburg et al., 2008). In this way, warfarin therapy leads to a decrease on the activity of the clotting factors II, VII, IX, and X, as well as the naturally endogenous anticoagulant proteins C and S, leading to a decrease on blood coagulation rate (Kuruvilla and Gurk-Turner, 2001). However, although warfarin treatment has been successfully used to control thromboembolic disorders, undesired side effects such as bleeding, swelling, bruising, articular pain or skin conditions have been reported as warfarin also prevents the γ-carboxylation of other VKDPs and might hamper the transcriptional activity of Pxr (Fernandez et al., 2014).

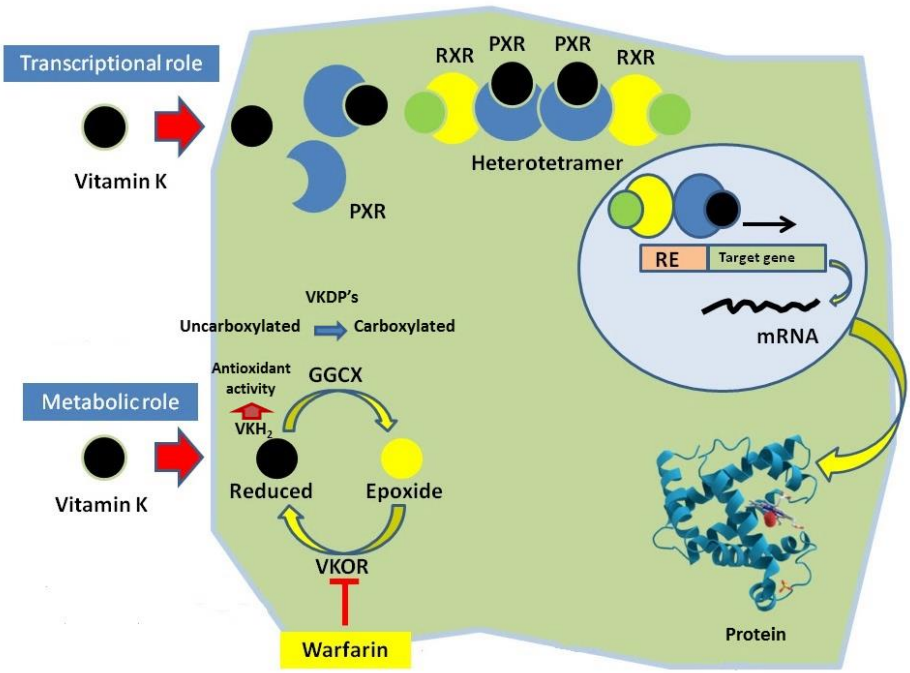

Figure 1.3. Vitamin K cycle and its metabolic and transcriptional roles. VK coming from dietary intake or glut microflora is first transformed to VKH_2 (reduced form has the antioxidant capacity). In one hand VKH_2 is used by the γ-glutamyl carboxylase (Ggcx) to convert glutamate into γ-carboxyl glutamate (Gla) residues in VK-dependent proteins; as a by-product VK epoxide. VK epoxide is then recycled to VK quinone by VK epoxide reductase (Vkor). VKH_2 is also involved in the antioxidant activity. Warfarin is a known inhibitor of

the VK recycling through its binding to Vkor. At the other VK is a ligand of the nuclear receptor Pxr. The activation of Pxr by VK, promote the formation of a heterodimer with retinoid acid receptor (Rxr). Then the formed complex will bind to Sxr responsive elements (Sxre) in the promotor or enhancer regions of target genes, activating their transcription and thus proteins synthesis.

1.6 VK deficiency

During pregnancy, anticoagulant therapy is recommended to women who use prosthetic heart valves and have thromboembolic conditions but also with history/symptoms of excessive levels of blood coagulation (How, 2004). However, this is problematic because since warfarin has a low molecular weight, it can pass through the placenta inducing spontaneous abortion, stillbirth, neonatal death, and a variety of congenital anomalies known as fetal warfarin syndrome (FWS) or warfarin embryopathy (WE; How, 2004; Sathienkijkanchai and Wasant, 2005). In WE the warfarin's teratogenic effects can occur when the fetus is exposed during either in embryonic (since fertilization until 8ª week) and fetal period (from 9ª week until the birth; Hou, 2004). However, the most critical period is between 6-9 weeks of gestation (reviewed in Sathienkijkanchai and Wasant, 2005). The effects comprise a wide range of manifestations such as dysmorphology in neonate with chondrodysplasia punctata (nasal hypoplasia and stippling of epiphyses), spine abnormalities, choanal atresia, laryngeal abnormalities, short neck, hypoplasia of distal phalanges, brachydactyly, short limbs and less frequently, abnormalities of the brain, eyes, and ears (Menger et al., 1997; Sathienkijkanchai and Wasant, 2005; Mehndiratta et al., 2010). Other manifestations in fetuses exposed to warfarin after the second or third trimester include optic atrophy, blindness, corneal opacity, deafness, microcephaly, hydrocephalus, epilepsy and mental retardation (reviewed in Sathienkijkanchai and Wasant, 2005).

Others conditions related with a deficiency of VK are known such as VK deficiency bleeding (VKDB) and VK deficiency embryopathy (Sutor et al., 1999; Shearer, 2009). VKDB is an acquired coagulopathy caused by a reduction of VK dependent coagulation factors below homeostatic levels, which is associated to intracranial hemorrhages in infants (Sutor et al., 1999; Shearer, 2009). VK deficiency embryophaty is a condition caused by a prenatal disorder in the VK metabolism, which is considered a phenocopy of WE (Menger et al., 1997). These conditions can be triggered by insufficient intake of VK, decreased gut flora, decreased VK absorption, or disruption of VK recycling

caused by mutations in Vkor and/or inhibited γ-carboxylation due to mutations in Ggcx enzymes (Menger et al., 1997; Greer, 2010; Takada et al., 2014). Several studies have demonstrated that mutations in Ggcx are responsible for visceral hemorrhages and a short life span (Zhu et al., 2007). Regarding to mutations in Vkor, Spohn et al., (2009) have demonstrated that homozygous Vkorc1-deficient mice developed normally until birth, but dyeing within 2-20 days after birth due to extensive, predominantly intracerebral hemorrhage resulted from a severe deficiency of γ-carboxylated clotting factors.

Although some information regarding the roles of VK and the signaling pathways controlled by Pxr at transcriptional level are known, the specific signaling pathways by which warfarin therapy during pregnancy induce WE in newborns is still not known.

1.7 Zebrafish

Animal models in biomedical research have been used to understand the mechanisms underlying vertebrate's development and pathogenesis of human diseases. In this sense, zebrafish (*Danio rerio*) has emerged as an excellent animal model, taking advantage over other ones, such as rodents and other mammalian species (reviewed by Lieschke and Currie, 2007). Zebrafish is a small freshwater teleost, with external fertilization, optical clarity during embryogenesis, rapid development, high reproductive rate and short life cycle. In addition, in the last years, genomic resources have been developed, including high density genetic maps for mapping induced mutations (Lieschke and Currie, 2007). In this sense, although zebrafish has been used mainly for developmental and molecular biology studies, teleosts are also suitable models for studying vertebrate skeletogenesis for both comparative (Witten and Huysseune, 2009) and evolutionary (Sire et al., 2009) purposes. Furthermore, zebrafish is a reliable tool in toxicology research as well as in drug discovery (Lieschke and Currie, 2007).

Previous works have demonstrated the expression and activity of Ggcx and its inhibition by warfarin exposure in zebrafish (Hanumanthaiah et al., 2001) and its teratogenicity and embryonic lethality under acute warfarin exposure (Weigt et al., 2012). Fernández et al., (2014) have characterized the effects of warfarin's long-term exposure during zebrafish exogenous feeding phase, and highlighted the two major up-stream pathways by which warfarin might affect normal development (VK-dependent protein γ-carboxylation rate and Pxr activation). More recently, Fernández et al., (2015) have

demonstrated that opposite VK status (induced VK deficiency by warfarin exposure and VK supplementation) was correlated with the altered expression of some of the molecular players of the VK cycle *in vitro*. The same authors also reported the gene expression patterns of *vkors* throughout larval development and in adult tissues in fish. Altogether indicate that zebrafish might be a good model to uncover the detailed mechanisms by which warfarin exposure during early development induce WE.

Chapter 2
Objectives

2. Objectives

The present study aimed at describing the effects of an induced VK deficiency through warfarin exposure in skeletogenesis and unveils the affected underlying skeletogenic pathways. Previous works have described the effects of an induced VK deficiency in zebrafish early development upon warfarin exposure. However, no reports have demonstrated the effects of VK deficiency in the skeletal development. In this work the effects of this deficiency in larval performance and skeletogenesis in zebrafish larvae exposed to warfarin during two critical periods of its development (0-2.5, embryonic stage; and 2.5-5 days post fertilization (dpf), endotrophic stage) will be evaluated. Larval performance, mineralization degree of the skeleton, skull structures length and gene expression of osteogenic markers will be analyzed at specific time points.

Chapter 3
Materials and methods

3. Materials and methods

3.1 Embryos rearing and fish maintenance

Zebrafish eggs were obtained from natural pairwise mating of wild type broodstock maintained in a ZebTec housing system (Tecniplast), being then collected and distributed in petri dishes (65-75 eggs per dish). Water parameters were maintained as follows: pH 7.6 ± 0.2; 700 mS conductivity; 7.8 mg L^{-1} dissolved oxygen; 14:10 hours light:dark photoperiod. In order to determine the effects of warfarin during the two key early developmental stages (embryonic and larval endogenous feeding phase), embryos or larvae were exposed to increasing concentrations of this VKA (0, 5, 25, 125 mg L^{-1}; named as Control, W5, W25, and W125, respectively) from 0 to 2.5 days post fertilization (dpf; embryonic development) and from 2.5 to 5 dpf (corresponding from hatching to mouth opening; endotrophic developmental stage; Fig. 3.1) in triplicate. After warfarin exposure, larvae were transferred to 500 ml tanks and raised until 16 dpf. From 4 dpf to the end of the trial zebrafish larvae were fed twice a day with newly hatched *Artemia* nauplii (AF strain INVE, 5-10 nauplii mL^{-1}), and a 50% water renewal every two days was done.

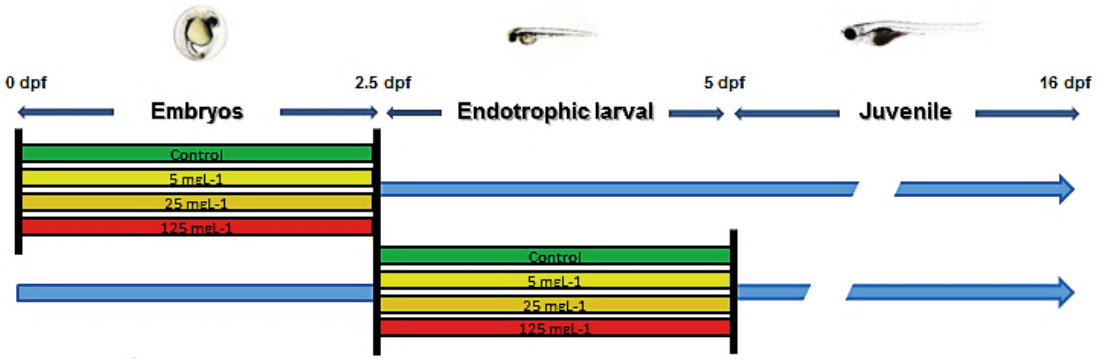

Figure 3.1. Schematic representation of zebrafish exposure to warfarin. Zebrafish embryos and larvae were exposed to increased levels of warfarin: 0 (Control), 5, 25 and 125 mg L^{-1} during embryonic and endotrophic stages. After warfarin exposure larvae were raised until 16 dpf.

3.2 Compound exposure

Warfarin (3-(α-acetonylbenzyl)-4-hydroxycoumarin sodium salt; Sigma-Aldrich) was dissolved in distilled water. Work solutions (5, 25 and 125 mg L^{-1}) were prepared for 30 ml of water from a stock of 10 mM.

3.3 Fish sampling

Fish from the different experimental groups were sampled at 3, 5, 7 and 16 dpf. Larvae were euthanized with a lethal dose of tricaine methanesulfonate (MS-222, Sigma-Aldrich) and washed with sterilized water. Larvae were then fixed in 1 ml of paraformaldehyde (PFA) 4% (pH 7.4), during 2h at room temperature (RT) and stored in 1ml of 100% ethanol (EtOH) until double staining procedure was performed, or in 1ml of TRIzol reagent (Qiagen) at -80 °C until RNA extraction.

3.4 Larval performance

Survival rate was calculated as the percentage of surviving fish at the end of the trial with respect to the initial number of fish minus the sampled larvae during embryonic or exogenous feeding larvae trials, respectively. Standard length of larvae, presence of hemorrhages, swimbladder inflation/development degree, pericardial aedema, yolk sac appearance and general larval morphology were evaluated under an MZ7.5 stereomicroscope (Leica Microsystems).

3.5 Skeletal development

In order to analyze the particular effects of warfarin exposure on the skeletal development and incidence of skeletal deformities, a modified whole amount alcian blue-alizarin S red double staining technique for bone and cartilage staining from Walker and Kimmel (2007) at 5, 7 and 16 dpf larvae was used (described in detail below). After staining, the skeletal development (percentage of structures non-, slightly- and mineralized) of cranial (basioccipital (bop), ceratohyal arches, ceratobranchial arches, cleithrum, operculum, parasphenoid) and axial structures (weberian, precaudal, vertebrae, fin vertebrae) was

assessed under a MZ7.5 stereomicroscope (Leica Microsystems). Skeletal structures were named according to Bird and Mabee (2003).

3.6 Whole mount double staining procedure

A modified whole mount alcian blue-alizarin S red double staining technique was used to stain larvae from 5, 7 and 16 dpf. In brief, after larvae were fixed with PFA (4% and pH 7.4), during 2 hours at RT, they were dehydrated in EtOH through a graded series of EtOH in water (25, 50, 75 and 100% v/v), during 10-30 minutes each. For the cartilage staining of the samples, they were treated with alcian blue Solution 0.02% (Stock solution 0.4%) with 80 mM chloride magnesium (in 70% EtOH) during 10-12 hours.

For bone staining, the samples were treated with a 0.005% alizarin red S solution in water for 1 hour (Stock solution 0.5%). Subsequently, larvae were bleached during at least 1 hour with a 1.5% hydrogen peroxide (H_2O_2) and 1% potassium hydroxide (KOH) solution. Finally, clearing of larvae to remove the excess of dye in soft tissues was done with 20% glycerol and 0.25% KOH solution for 4 hours, 50% glycerol and 0.25% KOH overnight (ON) at 4° C, 50% glycerol in water and 75% glycerol in water ON at 4 °C. Larvae were then stored in 100% glycerol at 4 °C. After staining, the mineralization status of the skeletal structures was evaluated.

3.7 Morphometric analysis

Cranial structures, such as meckel´s cartilage, ceratohyal, the first ceratobranchial arch and ethmoid plate were measured (length and width) as depicted in Figure 3.2. For this purpose, cranial structures of larvae previously double stained were manually dissected under a Stereo Discovery.V20 stereomicroscope (Zeiss) and placed in microscope slides. The structures were then photographed (AxioCam) in an Axio Imager.Z2 microscope (Zeiss) and analyzed using AxioVision image software.

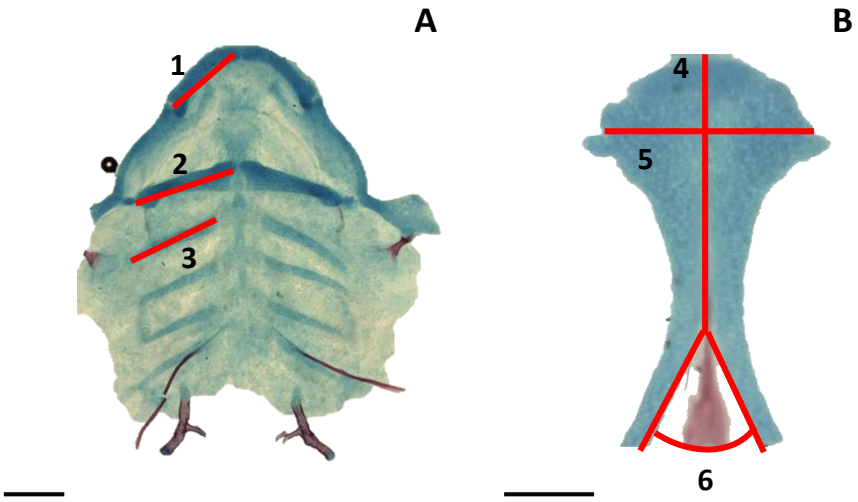

Figure 3.2. Schematic representation of the dissected and measured cranial structures in zebrafish larvae. Structures from the lower jaw, Meckel´s cartilage (1), ceratohyal arches (2), the first ceratobranchial arch (3; A) and from the upper jaw, ethmoid plate length (4), width (5) and angle (6; B) were measured in larvae exposed to increased levels of warfarin: 0 (Control), 25 (W25) and 125 mg L^{-1} (W125) during embryonic and larval stage. Scale = 100 µm.

3.8 RNA extraction

Total RNA was extracted from samples using TRIzol reagent (QIAGEN) as specified by the manufacturer. Briefly, samples were homogenized using seringes (18 and 20 G; TERUMO). The homogenate was then kept at room temperature (RT) during 5 minutes. After this step, phenol-chloroform (0.2 ml per ml of TRIzol) was added and vigorously agitated and kept at RT during 3 minutes. Samples were then centrifuged at 12000g, 4 °C during 15 minutes. At the end of this step three different phases were obtained. The upper aqueous phase (containing RNA) was passed to a new tube and subsequently isopropanol (0.5 ml per ml of TRIzol) was added. Tubes were then vortexed and incubated at RT during 10 minutes. A new centrifugation step was performed at 12000g, 4 °C during 10 minutes. The resulting supernatant was then removed and EtOH 75% was added (1 ml of 75% EtOH per ml of Trizol) to wash the pellet. A new centrifugation (7500g at 4 °C during 5 minutes) was done and EtOH 75% was removed. Diethylpyrocarbonate (DEPC) treated water (30 µL for first sampling points (3 and 5 dpf) and 100 µL for 16 dpf sampling

point) was added to eppendorfs and warmed (at 55 ºC) until RNA was dissolved. RNA quantification was determined measuring the optical density at 260 nm, using a Nanodrop (Thermo Scientific). Purity of RNA was established by the absorbance ratios 260/280 nm and 260/230 nm.

3.9 DNAse treatment and cDNA synthesis by Reverse Transcription (RT) reaction

The synthesis of cDNA was performed using the Moloney-murine leukemia virus (M-MLV) reverse transcriptase (200U/µL, Invitogen), according to manufacturer protocol. Briefly, RNA samples were treated with DNAse (RQ1 RNase-Free DNase; Promega). Next, the reaction was incubated for 10 minutes at 65 ºC. 500 ng of total RNA was supplemented with 1 µL oligo(dT) (500 µg/ml; Sigma-Aldrich) 1 µL dNTP's (10 mM, Invitrogen), 4 µL of First Strand buffer (5x, Invitogen) and 1 µL of DTT (0.1 M). This mixture was incubated during 3 minutes at 60 ºC, and then cooled 5 min at 4 ºC. To the resulting reaction 1 µL RNaseOUT (40U/µ, Invitrogen) and 1 µL of M-MLV reverse transcriptase was added. The reverse transcription reaction continued for 60 minutes at 37 ºC. Finally, samples were incubated during 5 minutes at 95 ºC to inactivate the reaction enzymes and stored at -20 ºC until use.

3.10 Gene cloning

For gene expression analysis and the evaluation of the efficiency of amplification by qPCR primers a different set of specific primers were designed (see Table 3.1) taking advantage of available genomic resources (NCBI and ENSEMBL).

Gene Name	**Access Number**	**Primer Name**	**Sequence (5'-3')**	**Bp size**
Col2a1a - ef	NM_131292.1	Forward	TTCACGGACTCTCCTGCTACTTGTG	458
		Reverse	GCTCGCCATCTCTCCCTCTTG	

Alp - ef	NM_201007.2	Forward	TTCCCCACGTCGCCCTCTCT	405
		Reverse	ACATGCTTCTCCGCCCACCC	
Runx2 - ef	NM_212862.1	Forward	GCACGGAGAGGGACTGACGG	357
		Reverse	AGGGCCACCACCTTAAACGC	
Osx - ef	NM_212863.1	Forward	GTTTCCCAGGACCCTTCGCT	498
		Reverse	GCAATCGCAAGAAGACCTCC	
Sox9a - ef	NM_131643.1	Forward	CCAGCGAACACTCAGGC	483
		Reverse	TGGTGATGGAGGGAAATGAAG	
Col2a1a - qPCR	NM_131292.1	Forward	CAGGAAGAGTTTGGCGGCTGT	81
		Reverse	GACACGGCACGGTTCTGGTT	
Alp - qPCR	NM_201007.1	Forward	TTCCTCTGCGGTGTCAAAGCCAA	184
		Reverse	AAGCAGCACTCGGGGTGGCAT	
Mgp - qPCR	NM_205640	Forward	TGTTGTTCTGGCTCTCGGTGCT	169
		Reverse	CACCTCCGCACGCCGCTC	
Bgp2 - qPCR	NM_001291889	Forward	CCAACTCCGCATCAGACTCCGCATCA	185
	.1	Reverse	AGCAACACTCCGCTTCAGCAGCACAT	
Runx2 - qPCR	NM_212862	Forward	CTCTCACGCAAACGGAGGACATACG	138
		Reverse	TGCATTCGAGTTCACGTCGTTCATCT	
Osx - qPCR	NM_212863.1	Forward	GCTAAGTCCAGGGCAGGCTCAG	115
		Reverse	CAATGGCGTGAAATCAGGAGTGTAAC	
Sox9a - qPCR	NM_131643.1	Forward	CGCCCACTCCTCCCACCACC	201
		Reverse	GACCGTTCGGCGGGAGGTATTG	
Grp1 - qPCR	JQ003911.1	Forward	CCATTCACTGCTCTCTCAACCACAA	128
		Reverse	GGCGGACAAAACAAGCAGACAG	
Rps18 - qPCR	NM_173234.1	Forward	AACACGAACATTGATGGAAGACG	255
		Reverse	ATTAGCAAGGACCTGGCTGTATTT	
B-actin2 - qPCR	NM_181601.4	Forward	GCAGAAGGAGATCACATCCCTGGC	322
		Reverse	CATTGCCGTCACCTTCACCGTTC	

Table 3.1. Gene names, access numbers (GenBank), primers, primer sequences and expected amplicon size (bp) used to perform the evaluation of the efficiency of qPCR primers and the relative gene expression quantification in zebrafish larvae exposed to warfarin during embryonic and endotrophic stages.

3.10.1 Determination of primers efficiency

To determine the efficiency of the qPCR designed primers (Table 3.1), a PCR reaction was done to amplify a fragment of the genes of interest, using zebrafish cDNA as template. In the amplification process, two different temperatures of annealing were used (65 and 68 ºC). For each PCR reaction it was added 1 µL of cDNA in a mix of 2.5 µL of Dream Taq buffer 10x, 2.5 µL of dNTPs (10mM), 1.5 µL of specific primers forward and reverse (10µM), 0.2 µL of Dream Taq Polymerase and miliQ water to a final volume of 25 µL. The PCR were performed under the following conditions: an initial denaturant step at 94 ºC for 5 minutes, followed by 35 cycles: 94 ºC during 30 seconds, 65 or 68 ºC during 30 seconds and 72 ºC during 30 seconds. PCR products of the expected size were confirmed by a gel electrophoresis.

3.10.2 Purified PCR product's ligation

In the ligation procedure the purified PCR products were inserted into pCR® II-TOPO® vector. In brief, the ligations on the pCR® II-TOPO® were performed following the manufacturer's instructions. 4 µL of the fresh PCR products were added to 1 µL of pCR® II-TOPO® vector and 1 µL of salt solution (6 µL final volume). The reaction was then incubated for 5 minutes at RT and then placed in ice.

3.10.3 Transformation of competent bacteria

The product obtained from the reaction of the previous step was inserted into E. coli - DH5α strain. In breaf, 4 µL of the pCR® II-TOPO® ligation reaction was added to a vial of E. coli. The tubes were then placed in ice for 30 minutes. Bacteria were incubated during 30 seconds at 42 °C (heat shock) to promote the DNA uptake. Under a Bunsen burner, 250 µL of a nutritive medium (SOC) was slowly added to the tubes in order to activate/potentiate E. coli. Next, bacteria were incubated during 1 hour at 37 °C with mechanical agitation (200 rpm). 100 µL of the bacterial suspension was pipetted and spread in a pre-warmed (at 37º C) LB agar plate containing ampicillin (100 µL ml^{-1} LB Agar) and X-GAL (40 µL per plate). The plates were then inverted and incubated at 37 °C ON. Individual and well defined white colonies (5 colonies per plate) were selected from

the plates and grown in 3.5 mL of LB medium with ampicillin (100 µL ml^{-1} LB) at 37 °C under constant mechanical agitation (200 rpm) ON, to promote bacterial colonies growth.

3.10.4 Screening of bacterial colonies by PCR

In order to confirm the presence of inserts of interest, a *polymerase chain reaction* (PCR) with the M13 primers and other with the specific primers for each gene was performed using 2 µL of the bacteria culture as DNA template. The M13 and the specific PCR primers will amplify the fragments of DNA that are inserted into the vector allowing us to confirm if the colonies are false or true positives. The primers (0.5 µL of 10 µM) were added in a mix with Dream Taq buffer 10x (2.5 µL), dNTPs (10 mM; 2.5 µL), Dream Taq Polymerase (0.2 µL) and DEPC water (17.8 µL). Finally, PCR products were analyzed by electrophoresis in an ethidium bromide (EtBr) agarose gel (1.2 – 2.0 %) in 1x TAE buffer and visualized under UV light in a High Performance UV Transluminator (UVP®).

3.10.5 Plasmid DNA extraction, purification and sequencing

Plasmid DNA extraction was performed manually. Briefly, the bacterial culture was centrifuge and the pellet was re-suspended in 100 µL of solution PI, which contains Tris-HCl (50 mM), ethylenediamine tetraacetic acid (10 mM; EDTA; prevents the activation of DNAses) and RNAse (100 µg mL^{-1}; responsible for degradation of RNA). 100 µL of a solution PII, which contains sodium dodecyl sulfate (SDS; a detergent that lyses the cells wall and denatures cellular proteins) and sodium hydroxide (200 mM; NaOH) was added and the mixture was incubated at RT for 5 minutes. After the incubation, 100 µL of solution PIII (containing Potassium acetate (3M)) was added to promote bacterial DNA and protein precipitation, due to the potassium acetate present in this solution. The mix was incubated in ice for 10 minutes and then centrifuged for 5 minutes at 13200 rpm. Plasmid DNA was precipitated after adding 2 volumes of 100% EtOH and washing with 2 volumes of 70% EtOH and re-suspended in 30 µL DEPC water. Plasmid DNA concentration and purity was determined by the absorbance ratios 260/280 and 260/230 nm using a Nanodrop 1000 spectrophotometer (Thermo Scientific). Finally, samples were sequenced at Centre of Marine Sciences (CCMAR) sequencing facility of the with the M13 F and M13 R primers.

3.11 Quantitative Real-Time PCR (RT-qPCR)

To quantify the expression of genes of interest, the cDNA resulting from the RT reaction was used as a template for qPCR. qPCR was performed on a Real-Time PCR system (Bio-Rad system) using gene-specific forward and reverse primers (Table 3.1). qPCR efficiency was close to 100% for all genes. All reactions were performed in triplicates in 96-well plates containing 10 ml of SsoFast EvaGreen Supermix (Bio-Rad), 0.5 ml of forward and reverse primers (10 µM), 7 ml of molecular biology grade water (Sigma), and 2 ml of a 1:10 dilution of cDNA template. Amplification parameters were as follows: 95°C for 1 min, followed by 40 amplification cycles at 95°C for 5 seconds and 65 °C for 10 seconds. A final dissociation reaction (melting curve) was performed with the following steps: 95 ºC for 15 seconds, 70 ºC for 1 minutes, and 15 seconds at incremental temperatures of 0.5 ºC until 95 ºC. A calibrator sample was included in each qPCR plate (Derveaux et al., 2010). Relative gene expression was determined according to Pfaffl et al. (2001) using cDNA from control larvae groups of both trials as reference samples, and set to one.

The suitability of 2 housekeeping genes (*β-actin2 and rps18*) was evaluated using NormFinder (Andersen et al. 2004) and BestKeeper (Pfaffl et al. 2004) algorithms. *Rps18* was selected as the best housekeeping gene.

3.12 Statistical analyses

Results are given as mean ± standard deviation. Differences among all experimental groups within each trial were identified by one-way ANOVA and T-test. Correlation between variables was evaluated using Pearson Product Moment Correlation test. When significant differences were detected in one-way ANOVA, Tukey multiple-comparison test was used to determine differences among experimental groups. In all cases, differences were considered to be significant when $P < 0.05$. All statistical analyses were done using GraphPad Prism 5.0 (GraphPad Software, Inc.).

Chapter 4
Results

4. Results

4.1 Survival rate and larval performance

Warfarin exposure during embryonic and endotrophic stages has promoted a wide range of effects in zebrafish larvae. Survival of the larvae exposed to increased levels of warfarin was clearly affected. Mortality of larvae exposed to gradual concentrations of warfarin increased overtime (Fig. 4.1A). However, while exposure during the embryonic stage (0-2.5 dpf) promoted a gradual increase in mortality when exposed to the highest concentration of warfarin (W125, 125 mg L^{-1}), and significantly higher from 4 dpf onwards (32.53 ± 7.09 %; one-way ANOVA, $P < 0.05$) when compared with the other groups (from 13.9 ± 2.55 to19.67 ± 1.70 %); exposure to warfarin during the endotrophic stage (2.5-5 dpf) showed quite low mortality until the 7 dpf. From 9 dpf onward, exposure to 125 mg L^{-1} induced a significant increase in mortality (15.65 ± 8.22 %; one-way ANOVA, $P < 0.05$) when compared with Control and lower concentrations (5 and 25 mg L^{-1}) of warfarin (from 1.67 ± 2.89 to 3.17 ± 1.4 %). The above mentioned mortality related with the exposure (concentration and developmental stage) to warfarin has been translated into a statistically different endpoint survival among experimental groups (Fig. 4.1B; one-way ANOVA, $P < 0.05$). Exposure to warfarin during the embryonic stage leads to a lower survival when treated with 125 mg L^{-1} (27.72 ± 5.75 %); while during the endotrophic stage (same concentration) showed a slighter effect on survival (61.29 ± 13.06 %).

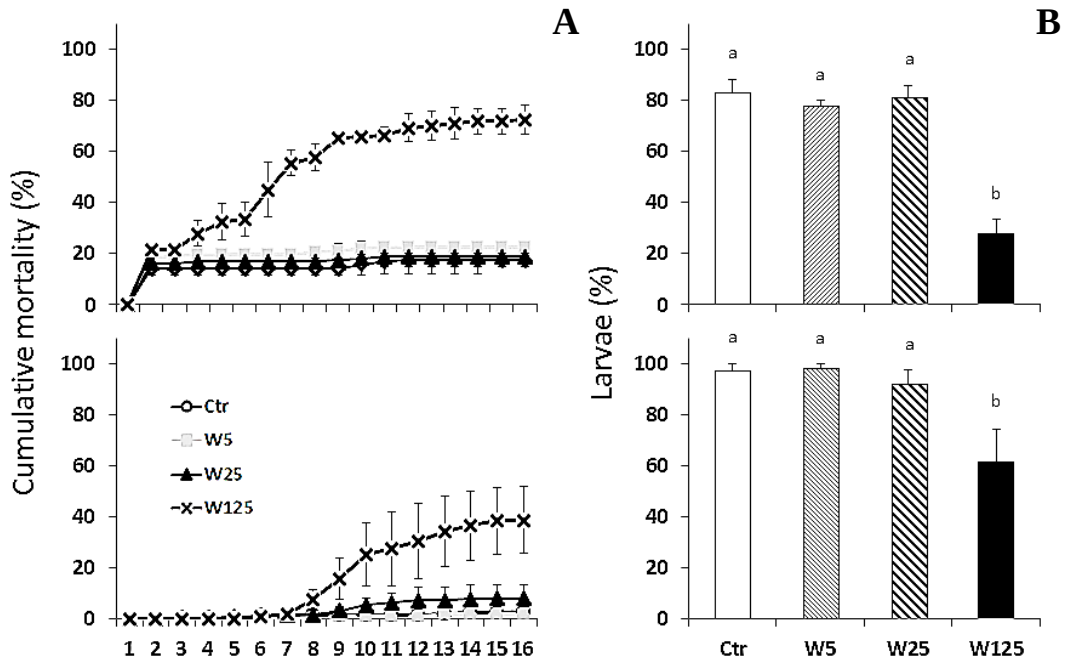

Figure 4.1. Cumulative mortality and endpoint survival rate of zebrafish exposed to increased concentrations of warfarin during the embryonic (upper images) and endotrophic stages (bottom images) at 16 dpf. Cumulative mortality (A) and endpoint survival (B) in zebrafish larvae exposed to increased levels of warfarin: 0 (Control), 5 (W5), 25 (W25) and 125 (W125) mg L^{-1}. Different letters at the top of histograms denote statistical significant differences among mean values from different experimental groups (one-way ANOVA, $P < 0.05$).

Larval performance was also compromised under an induced VK deficiency. Standard length at the first sampling point (3 dpf for embryonic and 5 dpf for endotrophic stage; Fig. 4.2A) was significantly lower when larvae were exposed to the highest concentration of warfarin (2.53 ± 0.01 mm in W125 larvae and ranging from 3.36 ± 0.02 to 3.31 ± 0.001 mm in Control, W5 and W25 groups, respectively; one-way ANOVA, $P < 0.05$). The same effect on standard length has been observed at the end of the experiment (16 dpf; Fig. 4.2B). At 16 dpf, larvae exposed to 125 mg L^{-1} during the embryonic stage were still significantly shorter (4.99 ± 0.18 mm) when compared with the larvae from the other warfarin treatments (from 8.21 ± 0.09 to 8.18 ± 0.09 mm; one-way ANOVA, $P < 0.05$), being those not statistically different to the one of Control larvae (8.19 ± 0.22 mm; one-way ANOVA, $P > 0.05$). However, when larvae were treated with warfarin during the endotrophic stage, they also showed a reduced growth in length compared to those not treated (Control), although the effect was slighter than in larvae exposed to warfarin during embryonic stage. In this case, W125 larvae showed the lowest standard length and significantly different to the larvae from the remaining experimental groups, showing W5 and W25 larvae intermediate values and also significantly different to those from Control larvae (7.43 ± 0.09 mm in Control group *versus* 6.99 ± 0.09, 7.10 ± 0.08, and 6.50 ± 0.15 mm in W5, W25 and W125, respectively; one-way ANOVA, $P < 0.05$).

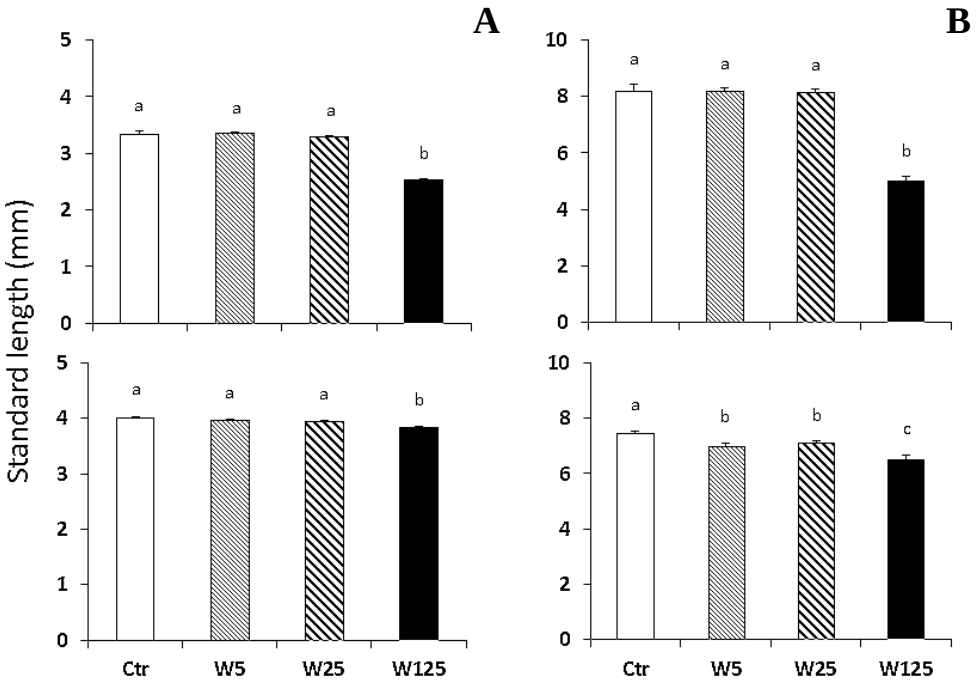

Figure 4.2. Standard length of larvae exposed to increased concentrations of warfarin during the embryonic (upper images) and endotrophic stages (bottom images) at different sampling points (3 and 16 dpf for embryonic stage treatment; 5 and 16 dpf for endotrophic stage treatment). Growth in standard length at 3 and 5 dpf (A) and growth in standard length at 16 dpf (B) in zebrafish larvae exposed to increased levels of warfarin: 0 (Control), 5 (W5), 25 (W25) and 125 (W125) mg L^{-1}. Different letters at the top of histograms denote statistical significant differences among mean values from different experimental groups (one-way ANOVA, $P < 0.05$).

In addition to the effects on survival and standard length, larvae exposed to warfarin also showed hemorrhagic events. At the first sampling point larvae exposed to 25 and 125 mg L^{-1} showed hemorrhages in abdominal region as well in the head (Fig. 4.3); however only the W125 group showed a significantly higher percentage with hemorrhages (60.83 ± 5.57 %; one-way ANOVA, $P > 0.05$). Similarly, although with a lower incidence (8.33 ± 0.01 %) comparing to the larvae treated during embryonic development, this feature was also seen in zebrafish exposed to highest warfarin concentration during the endotrophic stage. Furthermore, as occurred in embryonic stage, incidence of hemorrhages was not significantly different between untreated and larvae exposed to 5 and 25 mg L^{-1} of warfarin.

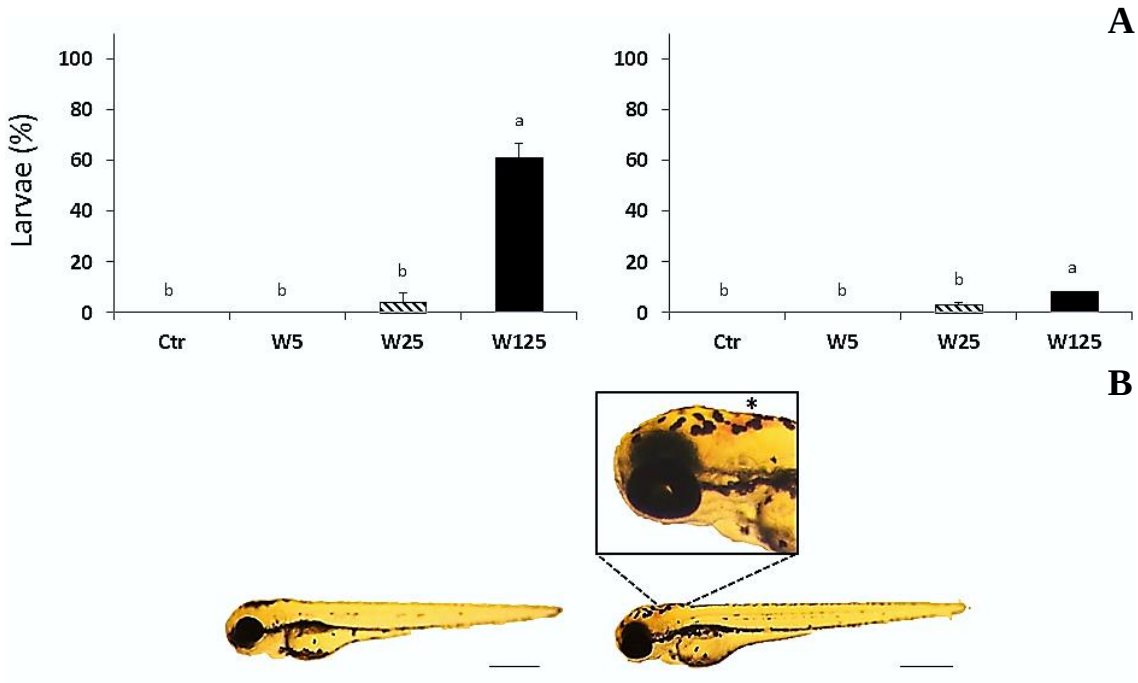

Figure 4.3. Percentage of larvae showing hemorrhages when exposed to increased concentrations of warfarin during the embryonic (left) and endotrophic stages (right) at 3 and 5 dpf, respectively (A). Larva treated with 5 mg L^{-1} with no hemorrhage *versus* larva treated with 25 mg L^{-1} showing cranial hemorrhage at 3dpf (B); asterisk indicates the local of hemorrhage. Levels of warfarin: 0 (Control), 5 (W5), 25 (W25) and 125 (W125) mg L^{-1}. Different letters at the top of histograms denote statistical significant differences among mean values from different experimental groups (one-way ANOVA, $P < 0.05$). Scale bar = 500 µm.

Yolk sac development was also compromised by warfarin exposure. Exposure to highest warfarin concentration during embryonic as well as during endotrophic development induced an opaque appearance of the yolk sac (Fig. 4.4). 54.44 ± 8.75 and 25.0 ± 11.79 % of the W125 larvae from embryonic and endotrophic development trials (respectively), showed this particular phenotype that has not been observed in Control, W5 and W25 treated larvae at 3 and 5 dpf sampling points.

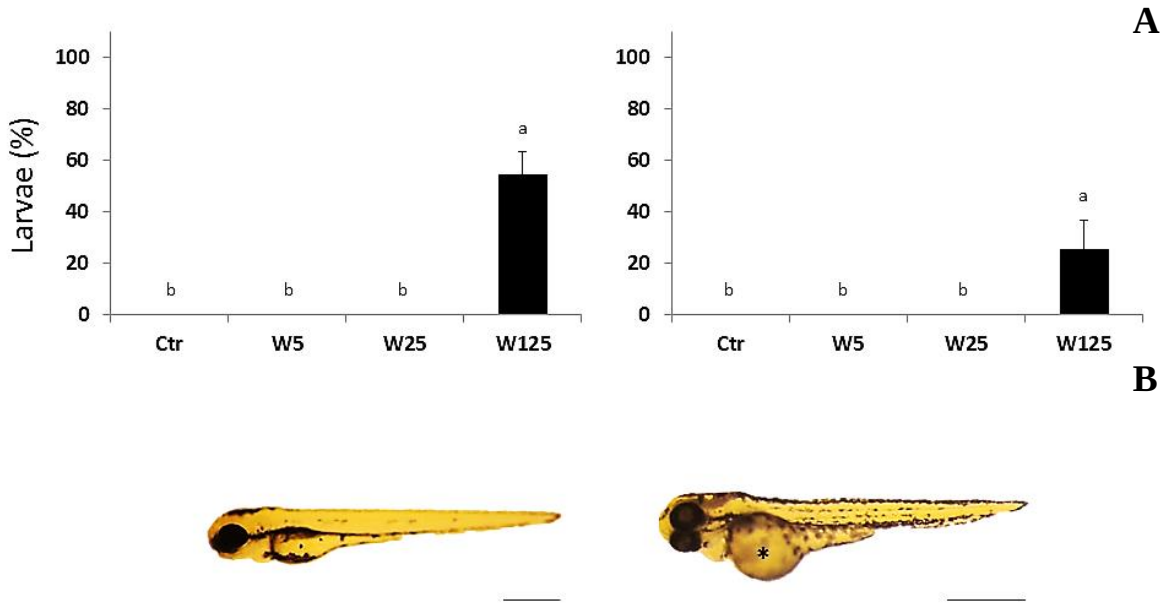

Figure 4.4. Percentage of larvae at 3 and 5 dph showing an opaque yolk sac when exposed to increased concentrations of warfarin during the embryonic (left image) and endotrophic stages (right image), respectively (A). Larva treated with 5 mg L^{-1} with no opaque yolk sac versus larva treated with 125 mg L^{-1} showing an opaque yolk sac at 3dpf (B); asterisk indicates yolk sac affected. Levels of warfarin: 0 (Control), 5 (W5), 25 (W25) and 125 (W125) mg L^{-1}. Different letters at the top of histograms denote statistical significant differences among mean values from different experimental groups (one-way ANOVA, $P < 0.05$). Scale bar = 500 µm.

Warfarin exposure also promoted the development of pericardial inflammation in zebrafish larvae (Fig. 4.5), with this effect being significant only in W125 exposed larvae and more pronounced when zebrafish were exposed to warfarin during embryonic rather than endotrophic (65.56 ± 15.48 and 11.11 ± 3.93 %, respectively; one-way ANOVA, $P > 0.05$) development. In fact, while pericardial inflammation was also observed in W5 and W25, larvae from the embryonic exposure, although in lower percentages (ranging 4.44 ± 3.14 to 8.89 ± 3.14 %), it was not found in W5 and W25 larvae from endotrophic exposure.

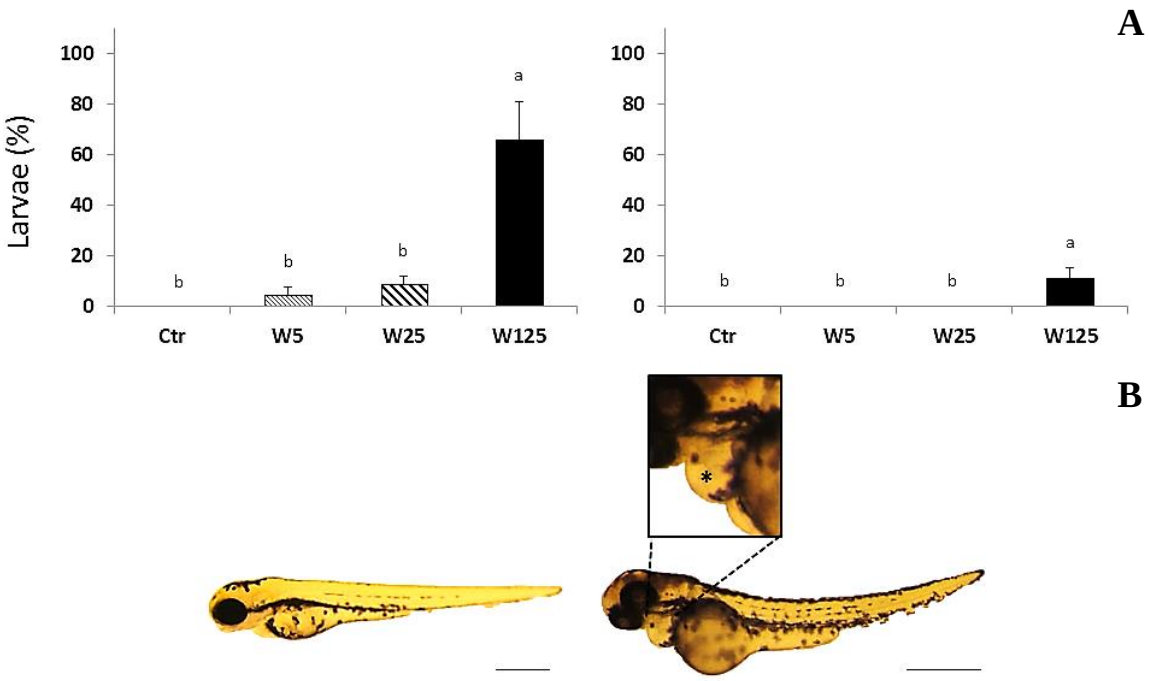

Figure 4.5. Percentage of larvae showing pericardial inflammation when exposed to increased concentrations of warfarin during the embryonic (left) and endotrophic stages (right) at 3 and 5 dpf, respectively (A). Larva treated with 0 mg L^{-1} with no pericardiac inflammation *versus* larva treated with 125 mg L^{-1} showing cardiac inflammation at 3dpf (B); asterisk indicates the pericardiac edema. Levels of warfarin: 0 (Control), 5 (W5), 25 (W25) and 125 (W125) mg L^{-1}. Different letters at the top of histograms denote statistical significant differences among mean values from different experimental groups (one-way ANOVA, $P < 0.05$). Scale bar = 500 µm.

The swimbladder development was also evaluated in zebrafish larvae. In this sense, zebrafish exposed to highest concentration of warfarin did not show a completely developed swimbladder (Fig. 4.6). At 16 dpf, only a little (12.73 ± 9.03 %; one-way ANOVA, $P > 0.05$) and a considerable percentage (46.50 ± 8.45 %; one-way ANOVA, $P > 0.05$) of larvae showed a fully developed swimbladder when exposed to 125 mg L^{-1} during the embryonic and endotrophic development, respectively. On the contrary, Control, W5 and W25 groups from both trials presented a high percentage of larvae with a normal swimbladder (with two lobules clearly differentiated).

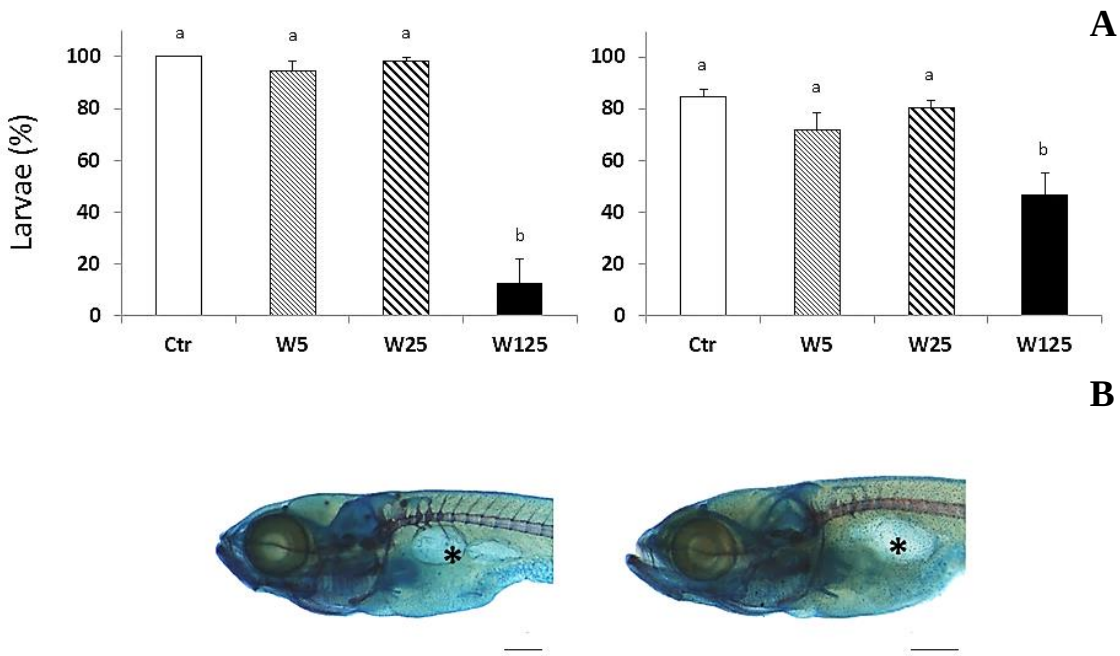

Figure 4.6. Percentage of larvae with the swimbladder fully developed when exposed to increased concentrations of warfarin during the embryonic (left image) and endotrophic stages (right image) at 16 dpf (A). Larva control with two swimbladder lobules clearly differentiated *versus* larva treated with 125 mg L^{-1} with only one swimbladder lobule formed (B); asterisk indicates the local of swimbladder in larvae. Levels of warfarin: 0 (Control), 5 (W5), 25 (W25) and 125 (W125) mg L^{-1}. Different letters at the top of histograms denote statistical significant differences among mean values from different experimental groups (one-way ANOVA, $P < 0.05$). Scale bar = 500 µm.

4.2 Zebrafish skeletogenesis

Skeletal development was also analyzed in larvae exposed to warfarin during embryonic and endotrophic stages, and particularly regarding the mineralization status of cranial and axial skeleton, and the morphometry of several cranial structures.

4.2.1 Cranial structures

The mineralization degree was analyzed in several structures of the cranium, where are included the basioccipital (bop), operculum, cleithrum, ceratohyal arches and parasphenoid. Regarding the morphometry, the meckel's cartilage, ceratohyal arches, the 1st ceratobranchial arch and the ethmoid plate were analyzed.

The mineralization degree was affected by warfarin exposure. While the bop was clearly visible in Control larvae, as it is showed fully mineralized; zebrafish exposed to increasing concentrations of warfarin during embryonic and endotrophic stages exhibited a less mineralized bop at 5 and 7 dpf, respectively (Fig. 4.7). When zebrafish were exposed to warfarin during the embryonic stage, the effect was more severe and none of the larvae treated with 125 mg L^{-1} had a mineralized bop at 5 dpf. Furthermore, this effect was still persistent at 7 dpf as a high percentage of larvae (72.22 ± 20.78 %; one-way ANOVA, $P > 0.05$) from W125 group showed a non-mineralized bop. Also, larvae from W25 group showed mineralization of bop affected at 5 dpf, with a considerable percentage (6.67 ± 9.43 %) presenting the structure non-mineralized and (60.00 ± 16.33 %) having a less mineralized bop. At 7 dpf, the mineralization degree between Control and the lower concentrations of warfarin was similar. When zebrafish were exposed to warfarin during endotrophic stage the effect was less evident; only a low percentage of larvae (22.98 ± 4.56 %) from W125 group showed no mineralization at 5 dpf, while these larvae presented a mineralization degree similar to the control at 7 dpf.

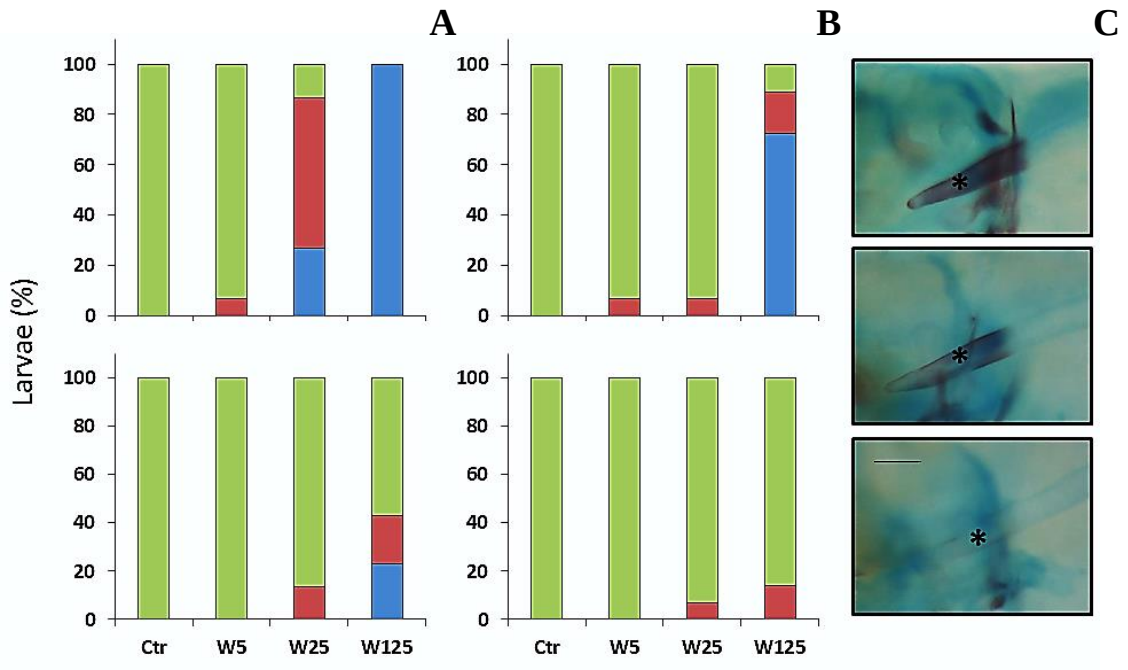

Figure 4.7. Percentage of zebrafish showing different mineralization degrees of the basioccipital (bop) when exposed to increased concentrations of warfarin during the embryonic (upper images) and endotrophic stages (bottom images). Percentage of larvae with different mineralization degree of bop at 5 (A) and 7 dpf (B) in zebrafish larvae exposed to increased levels of warfarin: 0 (Control), 5 (W5), 25 (W25) and 125 (W125) mg L^{-1}. Representative images of mineralized, less mineralized and not mineralized bop at 5 dpf (C).

Asterisks highlights bop in zebrafish larvae. Different colors in bars represent mineralization degree: blue, not mineralized; red, slightly mineralized; and green, mineralized. Scale bar = 100 µm.

Regarding to operculum, as occurred with the bop, the process of mineralization of this structure was affected, since a visible decrease in its mineralization on larvae exposed to the highest concentrations of warfarin in embryonic and endotrophic stages was found (Fig. 4.8). Zebrafish exposed to 125 mg L^{-1} of warfarin during the embryonic stage were the most affected group, showing no mineralization at 5 dpf. Larvae from W25 group also showed the operculum affected, since in a low percentage it was not (6.67 ± 9.43 %) or slightly mineralized (13.33 ± 18.86 %). At 7 dpf the effect was slighter, however all larvae from W125 group still presented the operculum less mineralized. When zebrafish were exposed to warfarin during endotrophic stage the effect was similar to the registered in embryonic one. Here, a significant percentage of larvae from W125 group (54.29 ± 3.40 %; one-way ANOVA, $P > 0.05$) showed the operculum not mineralized at 5 dpf; in contrast, the mineralization degree of larvae from Control and the lower concentrations of warfarin were similar. At 7 dpf, the effect was less visible, however larvae from W125 group still showing the operculum not full mineralized (69.44 ± 3.93 %; one-way ANOVA, $P > 0.05$).

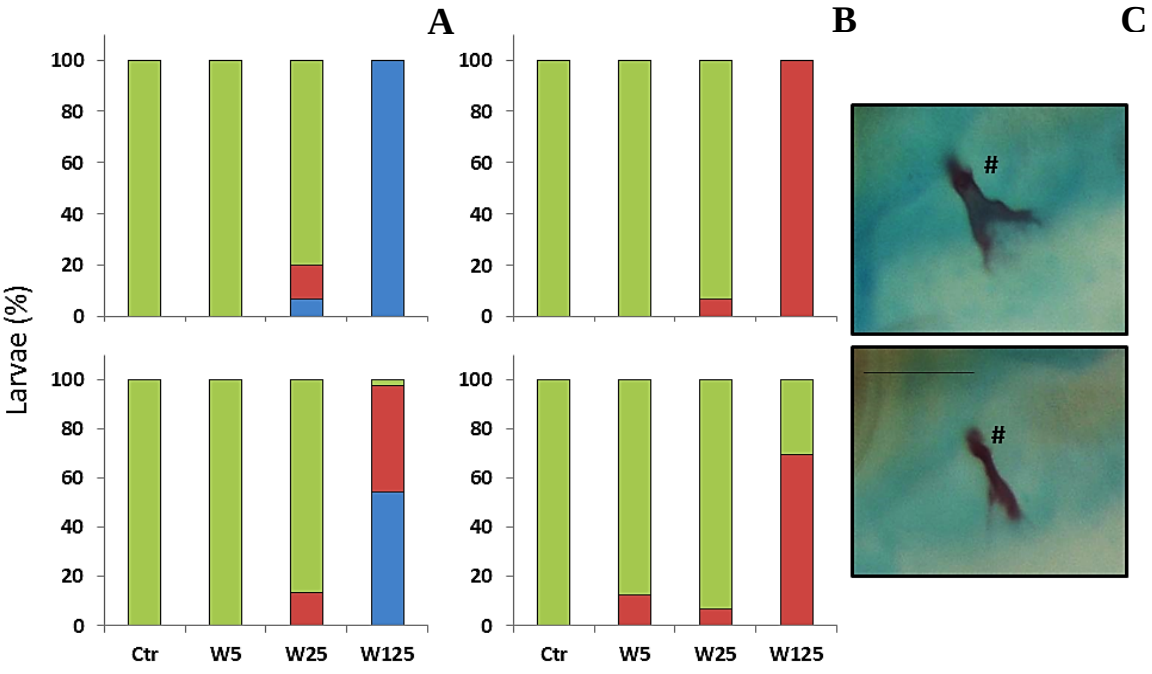

Figure 4.8. Percentage of zebrafish showing different mineralization degree of operculum when exposed to increased concentrations of warfarin during the embryonic (upper image) and endotrophic stages (bottom image). Percentage of larvae with different mineralization degree of operculum at 5 (A) and 7 dpf (B) in zebrafish larvae exposed to increased levels of warfarin: 0 (Control), 5 (W5), 25 (W25) and 125 (W125) mg L^{-1}. Representative images of mineralized and not mineralized operculum at 5 dpf (C). Cardinals highlights operculum in zebrafish larvae. Different colors in bars represent mineralization degree: blue, not mineralized; red, slightly mineralized; and green, mineralized. Scale bar = 100 µm.

The effect promoted by the exposition to warfarin in the cleithrum was also clear (Fig. 4.9). Larvae exposed to 125 mg L^{-1} of warfarin during the embryonic stage presented the most severe effect, and a significant percentage of larvae (88.89 ± 15.71 %; one-way ANOVA, $P > 0.05$) had the cleithrum not mineralized at 5 dpf. Larvae exposed to 25 mg L^{-1} also showed an effect, however less accentuated. A low percentage had the cleithrum not mineralized (6.67 ± 9.43 %) and a considerable percentage showed it slightly mineralized (33.33 ± 18.86 %). At 7 dpf the effect was smaller; the W125 group still showed the most severe effect, and all larvae had the cleithrum slightly mineralized; the mineralization degree between Control and the lower concentrations of warfarin was similar. When larvae were exposed to warfarin during endotrophic stage the effect was similar to the one seen in larvae exposed to warfarin during the embryonic stage; larvae treated with 125 mg L^{-1} were the most affected group, where a considerable percentage of larvae (45.20 ± 13.13 %; one-way ANOVA, $P > 0.05$) showing no mineralization in cleithrum at 5 dpf. At 7 dpf, the effect was less accentuated and all larvae showed mineralization in the cleithrum; in W125 group, the most affected group, a high percentage of larvae (69.44 ± 3.93 %; one-way ANOVA, $P > 0.05$) showed the cleithrum slightly mineralized, while a low percentage (30.56 ± 3.93 %; one-way ANOVA, $P > 0.05$) showed it fully mineralized; the lower concentrations of warfarin showed a similar mineralization degree when compared with Control.

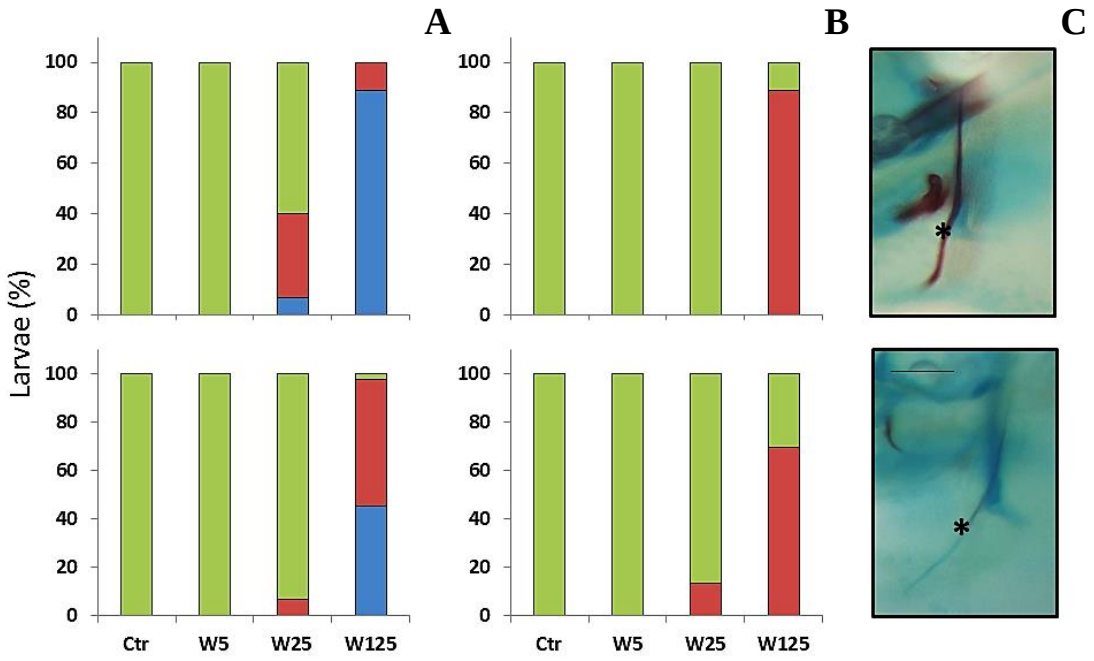

Figure 4.9. Percentage of zebrafish showing different mineralization degree of cleithrum when exposed to increased concentrations of warfarin during the embryonic (upper image) and endotrophic stages (bottom image). Percentage of larvae with different mineralization degree of cleithrum in zebrafish larvae at 5 dpf (A) and 7 dpf (B) exposed to increased levels of warfarin: 0 (Control), 5 (W5), 25 (W25) and 125 (W125) mg L^{-1}. Representative images of mineralized, less mineralized and not mineralized cleithrum at 5 dpf (C). Asterisks highlights cleithrum in zebrafish larvae. Different colors in bars represent mineralization degree: blue, not mineralized; red, slightly mineralized; and green, mineralized. Scale bar = 100 µm.

Mineralization degree of ceratohyal arches (Fig. 4.10) in larvae exposed to increasing concentrations of warfarin during embryonic and endotrophic stages was similar when compared to that of Control larvae at 5 dpf. In contrast, at 7 dpf, while larvae treated with 125 mg L^{-1} during embryonic stage showed no mineralization in ceratohyal, a significant percentage of larvae from Control and the lower concentrations of warfarin showed the structure slightly mineralized (80.0 ± 16.33, Ctr; 68.89 ± 24.55, W5 and 80.0 ± 0.0 %, W25). In contrast to this, when larvae were treated during the endotrophic stage, although a greater percentage of larvae from W125 group (94.44 ± 7.86 %) showed the ceratohyal not mineralized, the mineralization degree was similar to the registered in the other experimental groups.

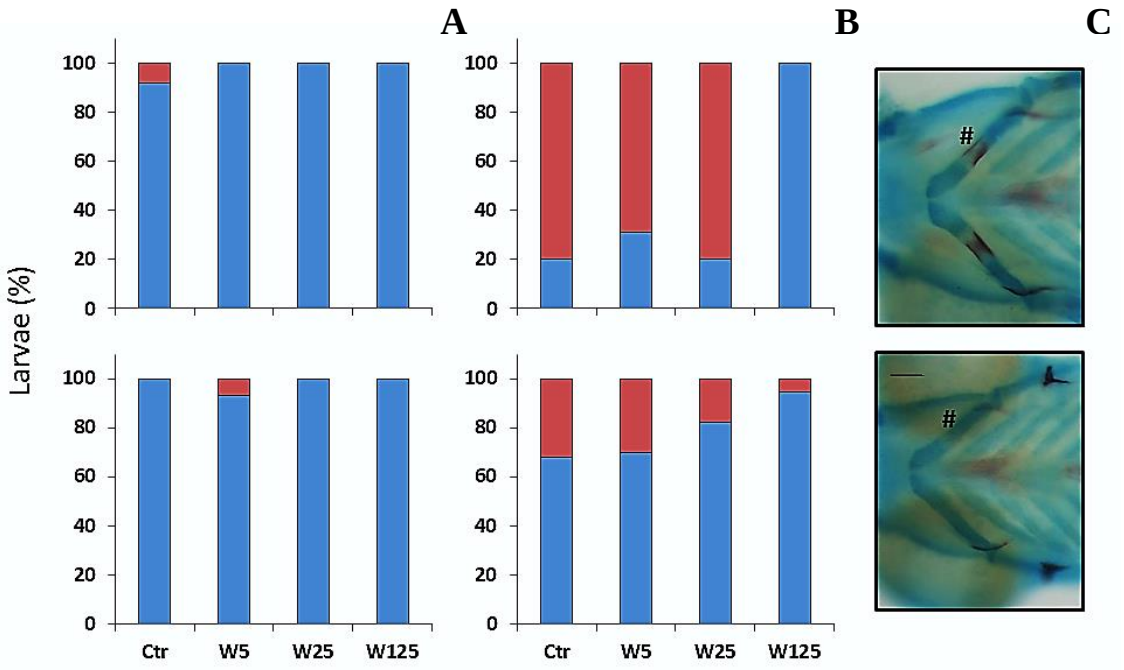

Figure 4.10. Percentage of zebrafish showing different mineralization degree of ceratohyal arches when exposed to increased concentrations of warfarin during the embryonic (upper image) and endotrophic stages (bottom image). Percentage of larvae with different mineralization degree of ceratohyal arches in zebrafish larvae at 5 dpf (A) and 7 dpf (B) exposed to increased levels of warfarin: 0 (Control), 5 (W5), 25 (W25) and 125 (W125) mg L^{-1}. Representative images of less mineralized and not mineralized ceratohyal arches at 5 dpf (C). Cardinals highlights ceratohyal arches in zebrafish larvae. Different colors in bars represent mineralization degree: blue, not mineralized; red, slightly mineralized. Scale bar = 100 µm.

The last structure analyzed in the cranium was the parasphenoid (Fig. 4.11). Here, the effect was similar to the one found in the previous analyzed structures. A deficit of mineralization in larvae exposed to the highest concentrations of warfarin (25 and 125 mg L^{-1}) was found when zebrafish were treated during embryonic and endotrophic stages at 5 and 7 dpf. When zebrafish were exposed to warfarin during the first stage, the effect was more severe in those treated with 125 mg L^{-1}, since no mineralization was detected at 5 dpf. The effect was smaller in larvae treated with 25 mg L^{-1} and a considerable percentage (40.0 ± 16.33 %) had the parasphenoid somewhat mineralized. At 7 dpf the effect was similar. Most of the larvae treated with 125 mg L^{-1} (72.22 ± 20.79 %; one-way ANOVA, $P > 0.05$) showed no mineralization in the parasphenoid, while similar mineralization degree was found between Control and the lower concentrations of warfarin. When zebrafish were exposed to warfarin during the endotrophic stage, the effect was similar to the one observed in the embryonic trial. Larvae treated with 125 mg L^{-1} were the most affected and

a significant percentage of larvae (62.63 ± 8.89 %; one-way ANOVA, $P > 0.05$) showed no mineralization at 5 dpf. Larvae treated 25 mg L^{-1} was also affected, however, in a slighter way since a greater percentage of larvae (60.0 ± 28.28 %) had the parasphenoid fully mineralized, and a considerable percentage (26.67 ± 24.94 %) had the parasphenoid at least slightly mineralized. At 7 dpf, the effect was less accentuated and all larvae have presented this structure mineralized. Nevertheless, W125 group was still the most affected, with a high percentage of larvae (75.0 ± 20.41 %; one-way ANOVA, $P > 0.05$) showing this structure less mineralized. In contrast, the degree of mineralization of Control and the lower concentrations of warfarin groups was similar.

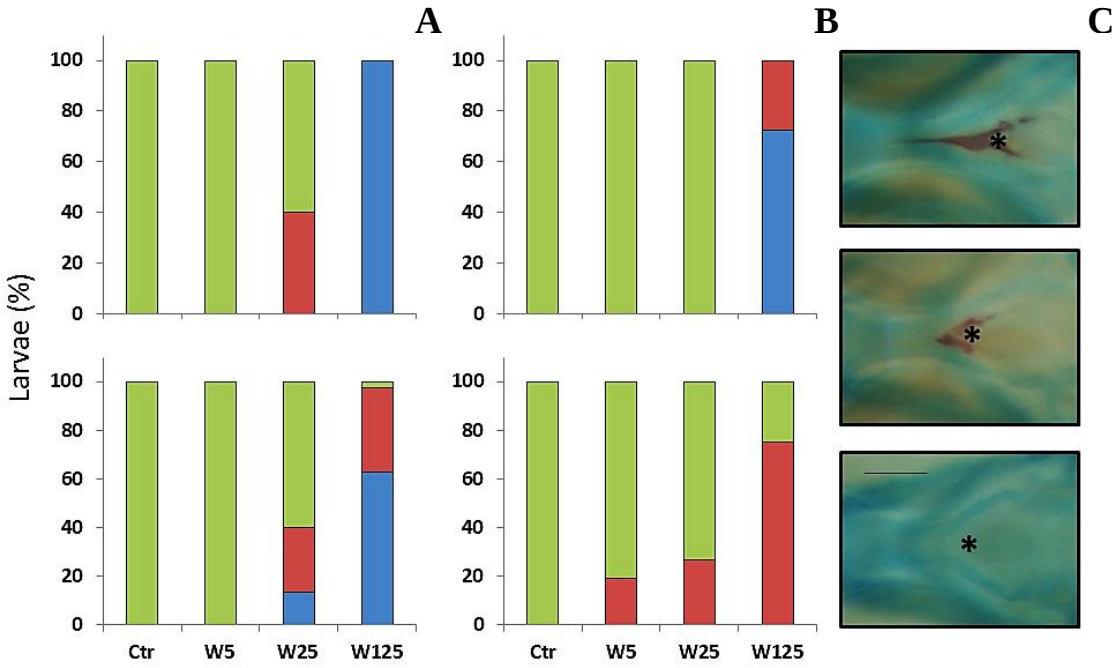

Figure 4.11. Percentage of zebrafish showing different mineralization degree of parasphenoid when exposed to increased concentrations of warfarin during the embryonic (upper image) and endotrophic stages (bottom image). Percentage of larvae with different mineralization degree of parasphenoid in zebrafish larvae at 5 dpf (A) and 7 dpf (B) exposed to increased levels of warfarin: 0 (Control), 5 (W5), 25 (W25) and 125 (W125) mg L^{-1}. Representative images of mineralized, less mineralized and not mineralized parasphenoid at 5 dpf (C). Asterisks highlights parasphenoid in zebrafish larvae. Different colors in bars represent mineralization degree: blue, not mineralized; red, slightly mineralized; and green, mineralized. Scale bar = 100 µm.

Besides the clear effect in mineralization, warfarin exposure has also compromised the morphometry of the endochondral structures present in the cranial region. One of these structures was the meckel's cartilage (Fig. 4.12). When larvae were treated with warfarin

during the embryonic stage, W125 group showed a significantly shorter structure at both 5 dpf and at 7 dpf (133.75 ± 5.42 and 173.48 ± 6.30 µm, respectively; one-way ANOVA, $P < 0.05$) when compared with the other treatments (ranging from 206.79 ± 5.80 to 197.69 ± 0.89 µm at 5 dpf, and 226.59 ± 12.44 to 209.58 ± 4.63 µm at 7 dpf). Similarly, larvae exposed to 125 mg L^{-1} during the endotrophic stage showed a significantly shorter structure at 5 dpf (157.54 ± 20.27 µm; one-way ANOVA, $P < 0.05$) when compared with the other treatments (ranging from 196.33 ± 8.02 to 191.45 ± 2.19 µm). At 7 dpf, larvae from W125 still showed a significantly shorter meckel's cartilage but only when compared with Control larvae (187.35 ± 2.13 *versus* 204.99 ± 9.09 µm, respectively; one-way ANOVA, $P < 0.05$), with larvae from W5 and W25 groups showing intermediate values (from 200.07 ± 6.97 to 199.6 ± 4.11 µm).

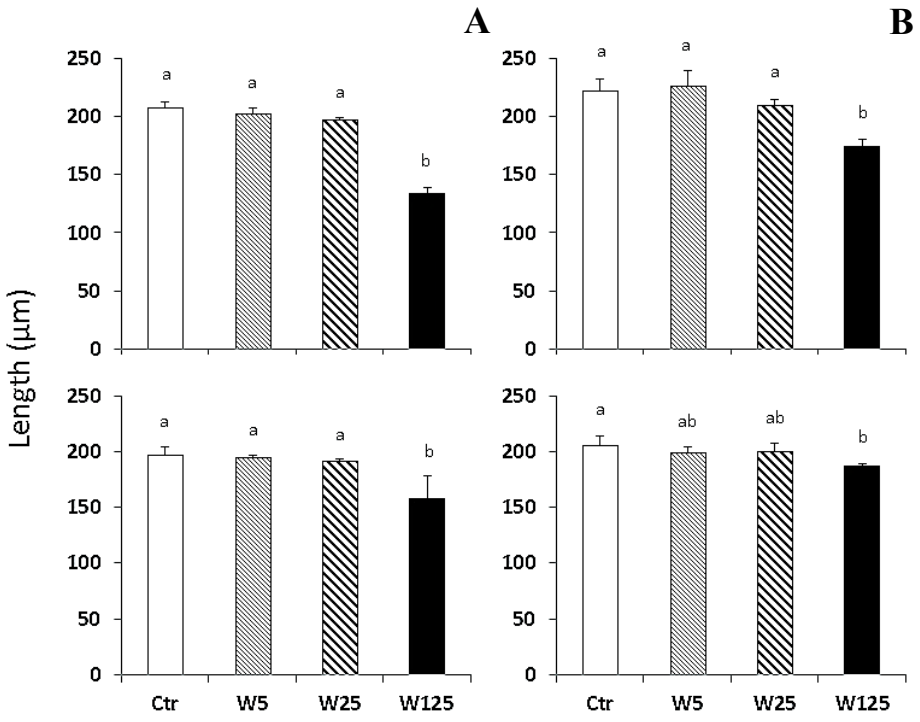

Figure 4.12. Mean length of meckel's cartilage in zebrafish exposed to increased concentrations of warfarin during the embryonic (upper image) and endotrophic stages (bottom image), respectively. Mean length of meckel's cartilage in zebrafish larvae at 5 dpf (A) and 7 dpf (B) exposed to increased levels of warfarin: 0 (Control), 5 (W5), 25 (W25) and 125 (W125) mg L^{-1}. Different letters at the top of histograms denote statistical significant differences among mean values from different experimental groups (one-way ANOVA, $P < 0.05$).

The ceratohyal length (Fig. 4.13) was also affected when zebrafish were exposed to increasing concentrations of warfarin at 5 and 7 dpf. As occurred in meckel's cartilage, the most severe effect was seen in larvae exposed to 125 mg L^{-1}. When zebrafish were exposed to this concentration during the embryonic stage a significant shorter structure was seen at 5 (172.77 ± 5.54 µm; one-way ANOVA, $P > 0.05$) and 7 dpf (207.16 ± 7.95 µm; one-way ANOVA, $P > 0.05$) comparing to the larvae from the other treatments (ranging from 253.06 ± 7.57 to 246.42 ± 3.08 µm at 5 dpf, and from 272.12 ± 4.12 to 256.34 ± 3.13 µm at 7 dpf). Furthermore, at 7 dpf, larvae exposed to 25 mg L^{-1} (256.34 ± 3.13 µm) presented an intermediate phenotype. A similar effect was found when larvae were exposed to the highest concentration during the endotrophic stage, since the ceratohyal arch was found significantly shorter at 5 (209.6 ± 15.79 µm; one-way ANOVA, $P > 0.05$) and 7 dpf (236.05 ± 6.55 µm; one-way ANOVA, $P > 0.05$) when compared to Control and the lower concentrations of warfarin (ranging from 243.13 ± 1.88 to 231.79 ± 2.85 µm at 5 dpf, and from 256.41 ± 5.76 to 243.53 ± 5.38 µm at 7 dpf).

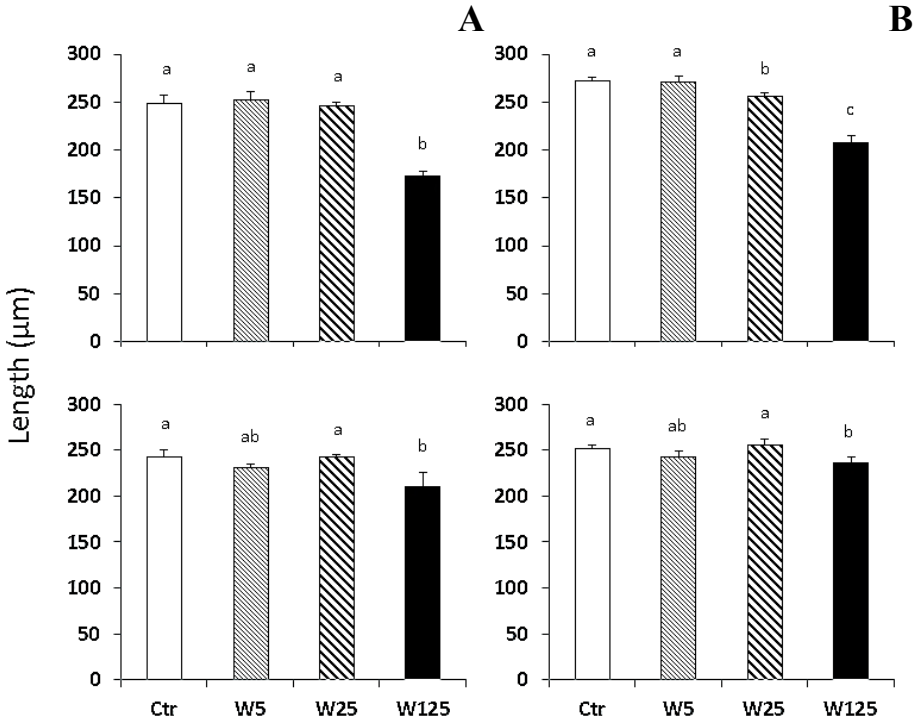

Figure 4.13. Mean length of ceratohyal arches in larvae exposed to increased concentrations of warfarin during the embryonic (upper image) and endotrophic stages (bottom image), respectively. Mean length of ceratohyal arches in zebrafish larvae at 5 dpf (A) and 7 dpf (B) exposed to increased levels of warfarin: 0 (Control), 5 (W5), 25 (W25) and 125 (W125) mg L^{-1}. Different letters at the top of histograms denote

statistical significant differences among mean values from different experimental groups (one-way ANOVA, $P < 0.05$).

The first ceratobranchial arch was also analyzed (Fig. 4.14). Larvae exposed to the highest concentration of warfarin showed the most severe effect at 5 and 7 dpf. When larvae were exposed 125 mg L^{-1} during the embryonic stage, a significant shorter structure was found (126.89 ± 10.37 µm; one-way ANOVA, $P < 0.05$) when compared with the larvae from the other treatments at 5 dpf (ranging from 226.93 ± 1.94 to 211.45 ± 5.69 µm) and similarly at 7 dpf. When larvae were exposed to increased levels of warfarin during the endotrophic stage, only larvae from W125 group showed a significant shorter first ceratobranchial at 5 and 7 dpf (168.34 ± 20.48 and 194.23 ± 9.33 µm, respectively; one-way ANOVA, $P < 0.05$) when compared with Control larvae.

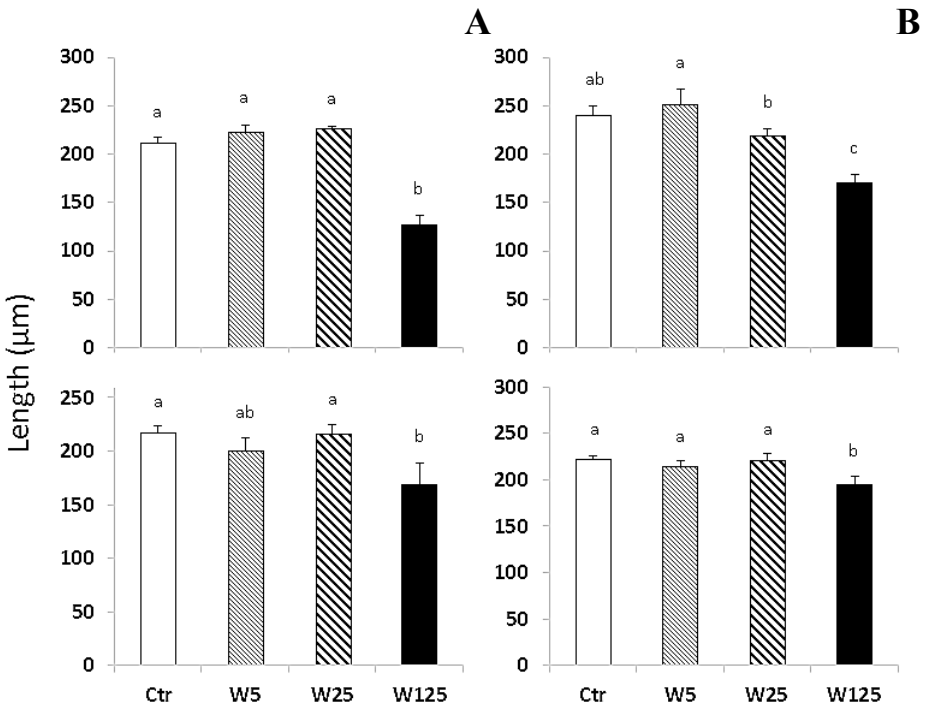

Figure 4.14. Mean length of the 1st ceratobranchial arch in larvae exposed to increased concentrations of warfarin during the embryonic (upper image) and endotrophic stages (bottom image), respectively. Mean length of the 1st ceratobranchial arch in zebrafish larvae at 5 dpf (A) and 7 dpf (B) exposed to increased levels of warfarin: 0 (Control), 5 (W5), 25 (W25) and 125 (W125) mg L^{-1}. Different letters at the top of histograms denote statistical significant differences among mean values from different experimental groups (one-way ANOVA, $P < 0.05$).

The width of the ethmoid plate (Fig. 4.15) was found affected. Larvae exposed to warfarin during the embryonic development, in particular to 125 mg L^{-1} at 5 dpf and at 7 dpf had a significantly narrower structure (117.51 ± 7.97 µm; one-way ANOVA, $P > 0.05$), comparing with the other experimental groups (range from 199.24 ± 1.80 to 189.64 ± 4.34 µm). When treated during the endotrophic stage, larvae from W125 group showed a significant reduction in width (162.02 ± 14.74 µm; one-way ANOVA, $P > 0.05$) when compared with the lower concentrations of warfarin, being the effect visible at 5 dpf. At 7 dpf, the effect found was less evident; however, larvae exposed to 125 mg L^{-1} still had a significantly narrower structure (180.02 ± 9.51 µm) compared to that found in Control larvae.

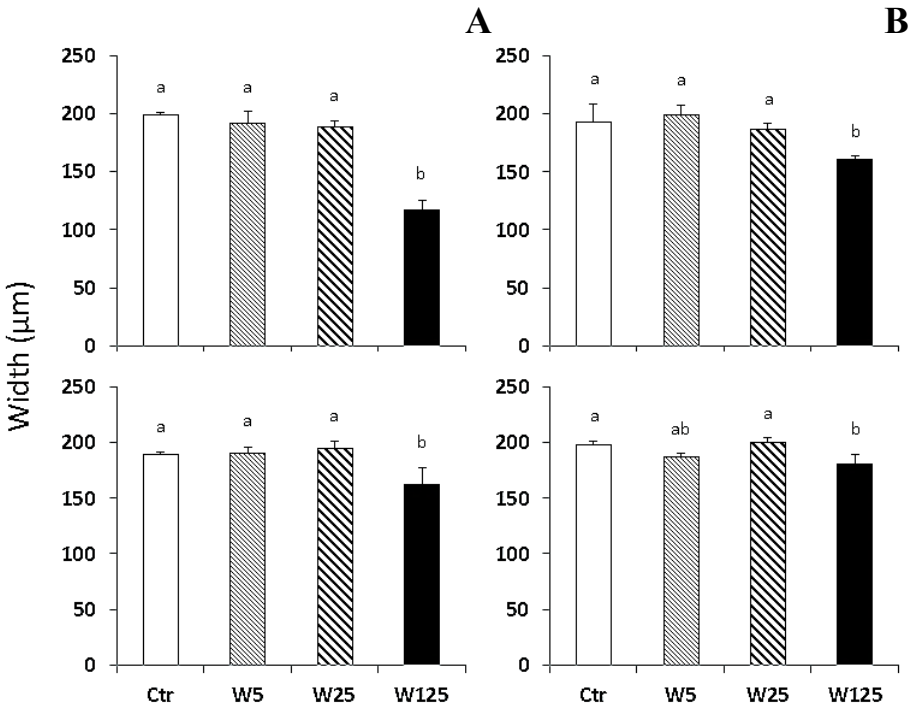

Figure 4.15. Mean width of the ethmoid plate in larvae exposed to increased concentrations of warfarin during the embryonic (upper image) and endotrophic stages (bottom image), respectively. Mean width of the ethmoid plate in zebrafish larvae at 5 dpf (A) and 7 dpf (B) exposed to increased levels of warfarin: 0 (Control), 5 (W5), 25 (W25) and 125 (W125) mg L^{-1}. Different letters at the top of histograms denote statistical significant differences among mean values from different experimental groups (one-way ANOVA, $P < 0.05$).

Regarding to the length of the ethmoid plate (Fig. 4.16), larvae exposed to 125 mg L^{-1} were the most affected, being the effect more severe when they were exposed to

warfarin during the embryonic stage. At 5 dpf, larvae treated during this stage showed an ethmoid plate significantly shorter (129.36 ± 3.87 µm; one-way ANOVA, $P > 0.05$) when compared with the other experimental groups (ranging from 253.04 ± 11.96 to 224.74 ± 8.82 µm). At 7 dpf, a similar effected was found, with larvae exposed to 125 mg L^{-1} having an ethmoid plate still significantly shorter (188.64 ± 27.94 µm; one-way ANOVA, $P > 0.05$). Furthermore, larvae treated 25 mg L^{-1} showed an intermediate phenotype between Control and W125 larvae. Exposure to warfarin during the endotrophic stage promoted similar effect in larvae, although less accentuated. At 5 dpf, W125 group was the most affected, with larvae showing a significant shorter structure (178.15 ± 26.68 µm; one-way ANOVA, $P > 0.05$) compared to that of the Control larvae. At 7 dpf, a similar effect was found with W125 larvae showing a significantly shorter structure (204.43 ± 5.23 µm; one-way ANOVA, $P > 0.05$) compared to the other groups.

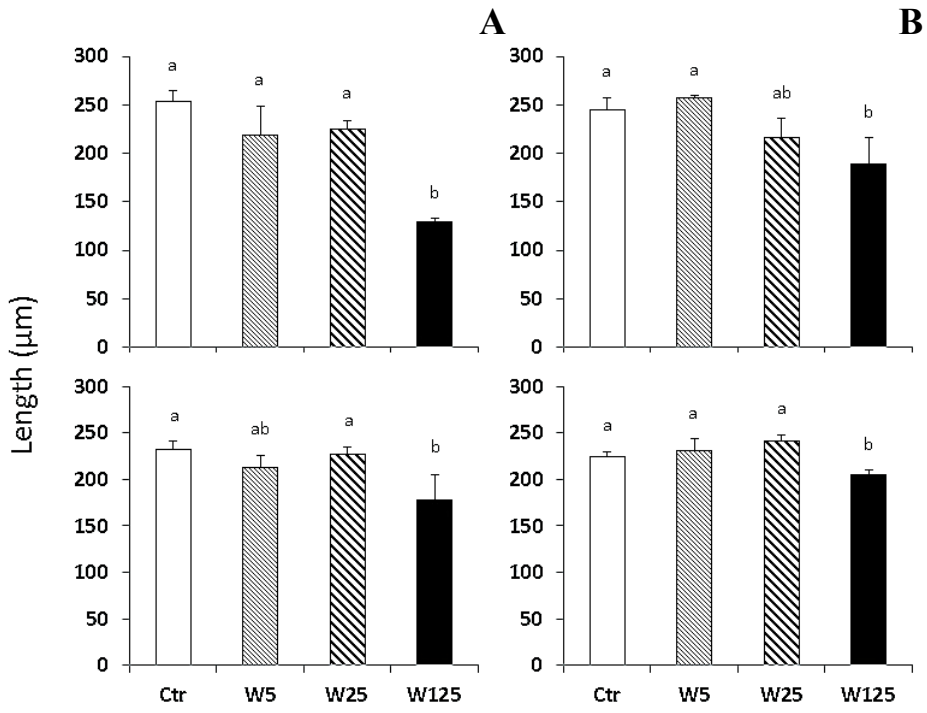

Figure 4.16. Mean length of the ethmoid plate in larvae exposed to increased concentrations of warfarin during the embryonic (upper image) and endotrophic stages (bottom image), respectively. Mean length of the ethmoid plate in zebrafish larvae at 5 dpf (A) and 7 dpf (B) exposed to increased levels of warfarin: 0 (Control), 5 (W5), 25 (W25) and 125 (W125) mg L^{-1}. Different letters at the top of histograms denote statistical significant differences among mean values from different experimental groups (one-way ANOVA, $P < 0.05$).

Unlike the previous parameters, only larvae treated with warfarin during the embryonic stage and with the highest concentration were significantly affected regarding the angle formed by the ethmoid plate (Fig. 4.17). The larvae analyzed showed a larger angle at 5 dpf (80.70 ± 13.96 °; one-way ANOVA, $P > 0.05$) and 7 dpf (65.50 ± 5.79 °; one-way ANOVA, $P > 0.05$) when compared to the rest of the treatments at 5 dpf (48.81 ± 3.93 °, Ctr; 49.77 ±1.81 , W5; 51.69 ± 1.43 °, W25); and at 7 dpf (49.52 ± 3.99 °, Ctr; 50.69 ± 4.47, W5; 51.19 ± 0.99 °, W25).

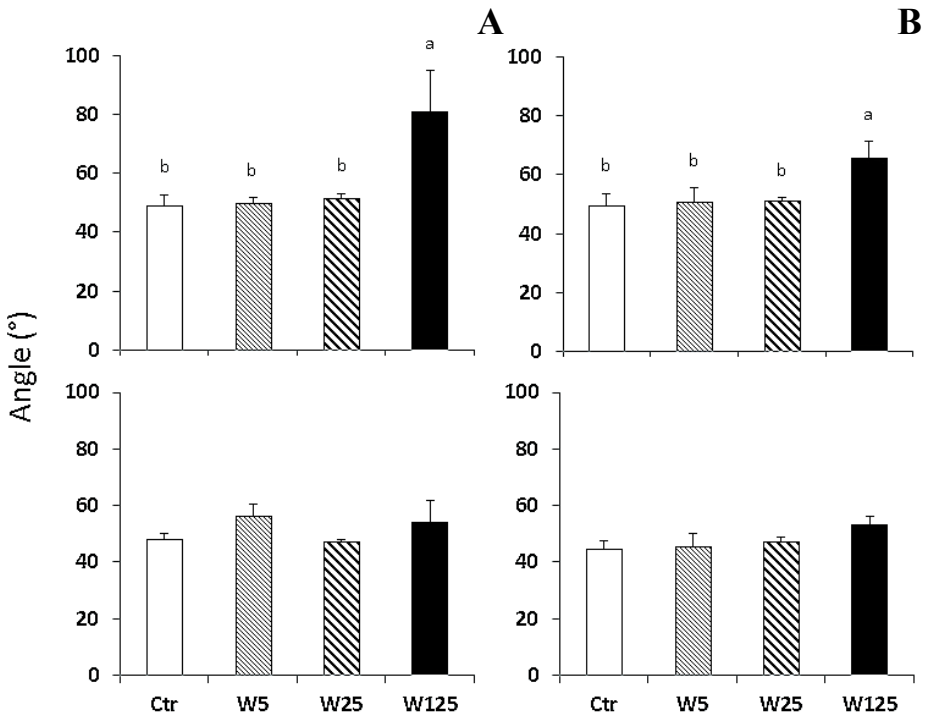

Figure 4.17 Mean angle of the ethmoid plate in larvae exposed to increased concentrations of warfarin during the embryonic (upper image) and endotrophic stages (bottom image), respectively. Mean angle of the ethmoid plate in zebrafish larvae at 5 dpf (A) and 7 dpf (B) exposed to increased levels of warfarin: 0 (Control), 5 (W5), 25 (W25) and 125 (W125) mg L^{-1}. Different letters at the top of histograms denote statistical significant differences among mean values from different experimental groups (one-way ANOVA, $P < 0.05$).

4.2.2 Axial skeleton

As in the cranial region, mineralization in axial skeleton (Fig. 4.18) was also found to be affected by exposure to warfarin at the end of the experiment (16 dpf). However, a clear decrease of mineralization was only visible in larvae exposed to 125 mg L^{-1}. In this

sense, when zebrafish were treated during the embryonic stage, the most affected one, a significantly lower percentage of larvae had mineralized the vertebrae. In contrast, although larvae treated during the endotrophic stage were also affected, most of them exposed to the highest concentration showed a normal mineralization pattern in most of the vertebra; only a low percentage of larvae showed a normally mineralization on the last vertebrae.

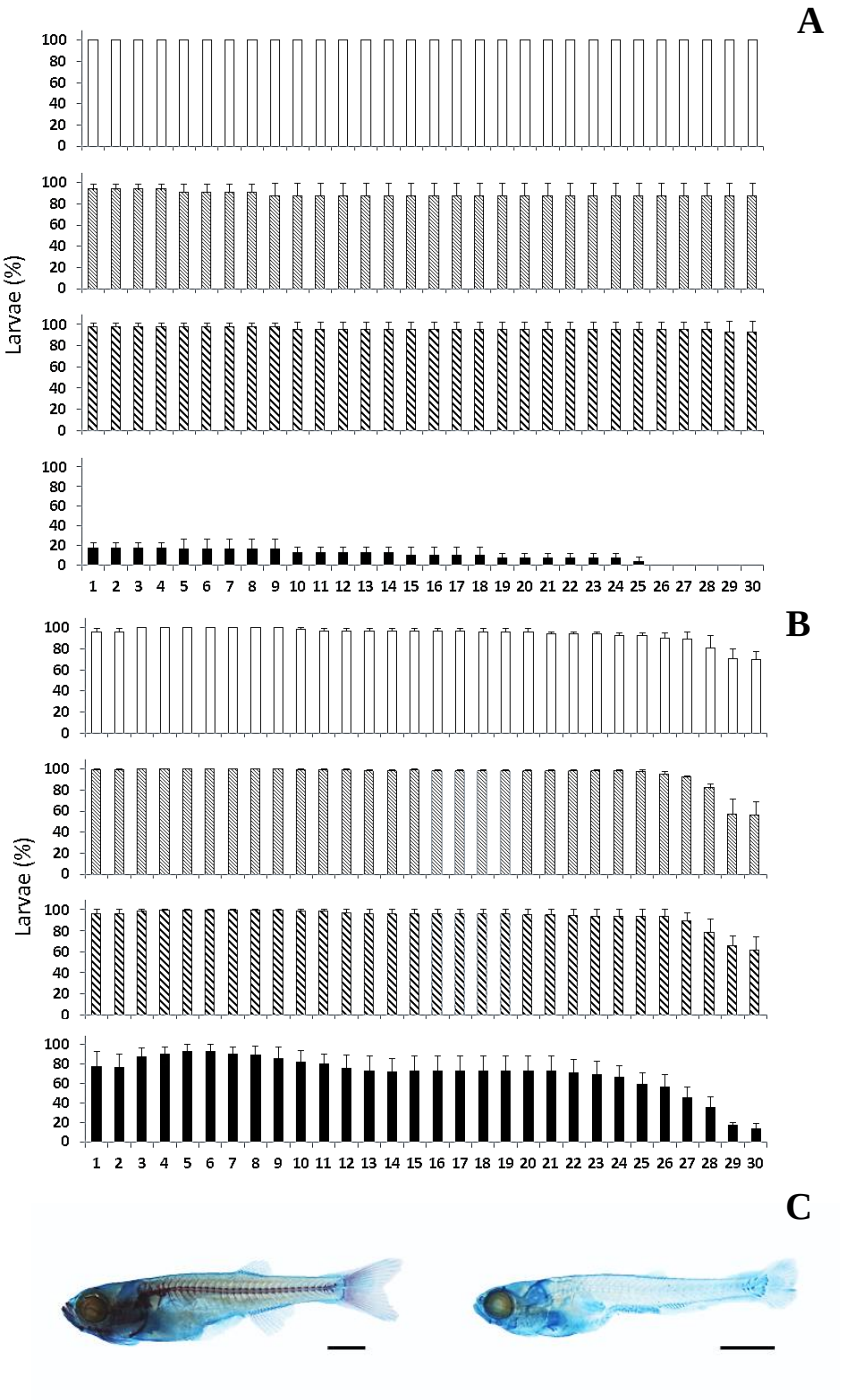

Figure 4.18. Percentage of zebrafish showing different mineralization of vertebrae when exposed to increased concentrations of warfarin. Percentage of larvae with vertebrae mineralized in zebrafish larvae at 16 dpf exposed to increased levels of warfarin during the embryonic (A) and endotrophic stages (B): 0 (Control), 5 (W5), 25 (W25) and 125 (W125) mg L^{-1}. Representative images of mineralized and non-mineralized axial skeleton at 16 dpf (C). Scale bar = 1mm.

4.3 Gene expression

To better understand the mechanisms that regulate skeletal formation in zebrafish under exposure to warfarin during the embryonic and endotrophic stages, expression levels of genes related to skeletogenesis (*sox9a*, *runx2*, *osx*, *col2a1*, *grp1*, *alp*, *mgp* and *bgp*) were determined by qPCR in larvae from Control, W25 and W125 at 3 dpf in embryos exposed to warfarin during the embryonic stage, at 5 dpf in larvae exposed to warfarin during the endotrophic stage and in Control and W125 larvae at 16 days when they were exposed to warfarin during the endotrophic stage.

In larvae exposed to warfarin during the embryonic stage only *sox9a* was affected regarding to the transcriptional factors controlling skeletogenesis at 3 dpf; being only significantly down regulated in larvae from W125 group (*t*-test, $P < 0.05$; Fig. 4.19). While the expression of alkaline phosphatase (*alp*) was not found to be altered in larvae exposed to increased levels of warfarin; two genes encoding for extracellular matrix proteins *col2a1a* and *grp1* were found significantly down-regulated. In particular, while *col2a1a* was only significantly down-regulated in larvae from W125 group with respect to larvae from Control group, *grp1* was found to be down-regulated in larvae from W25 and W125 groups (one-way ANOVA, $P < 0.05$).

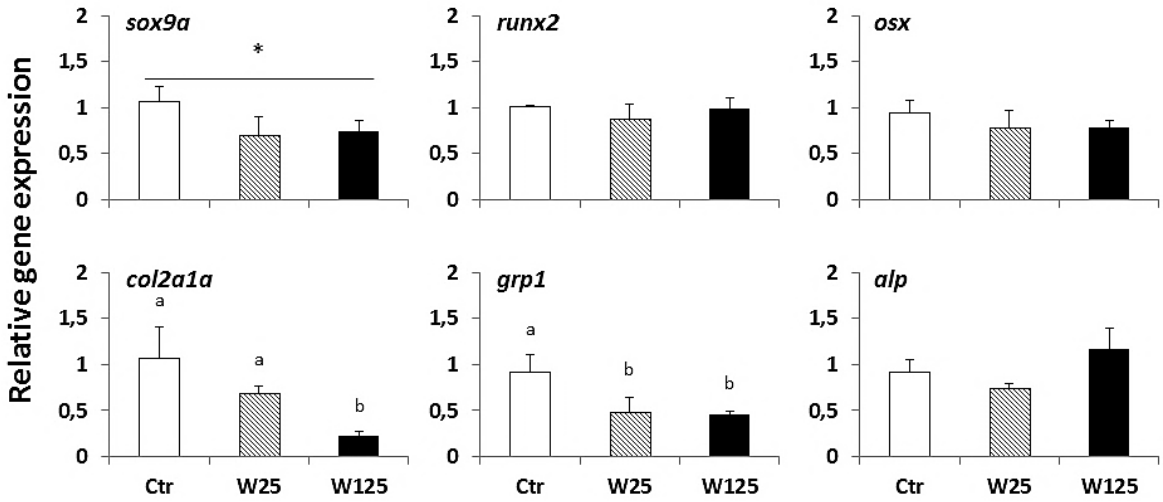

Figure 4.19. Relative expression of *sex determining region Y-box 9a*, *runt-related transcription factor 2*, *osxterix*, *collagen type 2*, *gla-rich protein 1* and *alkaline phosphatase* genes in zebrafish at 3 dpf upon exposure to warfarin during embryonic stage: 0 (Ctr) and 25 (W25) and 125 (W125) mg L^{-1}. Transcript levels were determined by qPCR from 3 biological replicates (3 technical replicates per biological replicate) and normalized using *Rps18* housekeeping gene. An asterisk denotes statistical difference among two groups by *t*-test, while different letters statistical difference among experimental groups by one-way ANOVA ($P < 0.05$). Relative gene expression was determined using cDNA from control larvae groups as reference samples, and set to one. *Sox9a*, *sex determining region Y-box 9a*; runx2, *runt-related transcription factor 2*; *osx*, *osterix*; *col2a1a*, *collagen type 2*; *grp1*, *gla-rich protein 1*; *alp*, *alkaline phosphatase*.

At 5 dpf (Fig. 4.20), *osx* expression was significantly decreased in larvae exposed to the highest concentration of warfarin (W125) compared to that of larvae from the Control group (one-way ANOVA, $P < 0.05$). Although *col2a1a* gene expression was not statistically different among experimental groups, a negative correlation between warfarin concentration and its level of expression (Pearson product-moment correlation; $P = 0.034$; $R^2 = 0.555$) was found. Also, *grp1* and *alp* were significantly affected, being down-regulated in W125 larvae when compared to Control larvae (*t*-test and one-way ANOVA, respectively; $P < 0.05$).

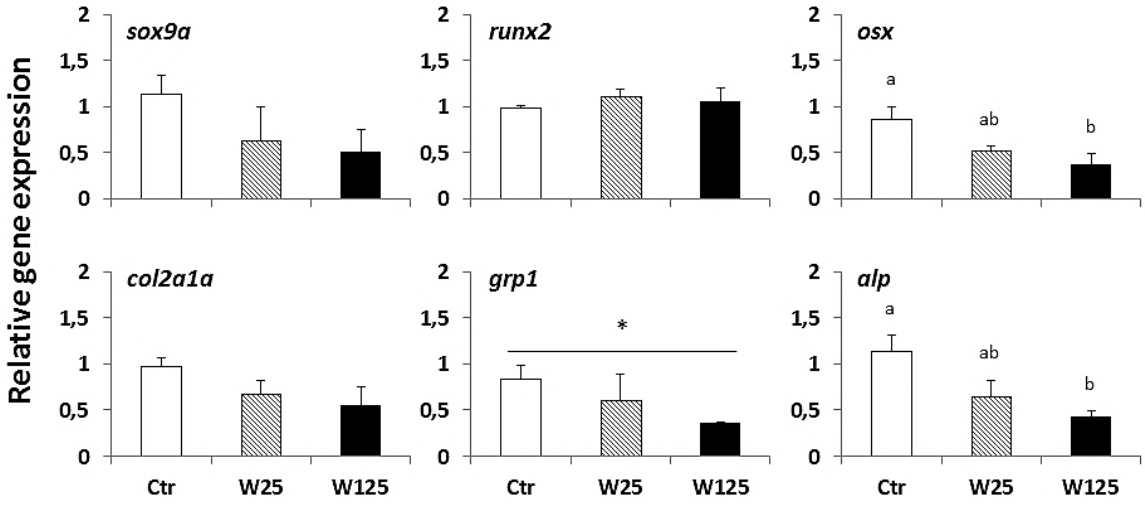

Figure 4.20. Relative expression of *sex determining region Y-box 9a*, *runt-related transcription factor 2*, *osxterix*, *collagen type 2 alpha 1a*, *gla-rich protein 1*and *alkaline phosphatase* genes in zebrafish larvae at 5 dpf upon exposure to warfarin during endotrophic stage: 0 (Ctr) and 25 (W25) and 125 (W125) mg L^{-1}. Transcript levels were determined by qPCR from 3 biological replicates (3 technical replicates per biological

replicate) and normalized using *Rps18* housekeeping gene. An asterisk denotes statistical difference among two groups by *t*-test while different letters statistical difference among experimental groups by one-way ANOVA ($P < 0.05$). Relative gene expression was determined using cDNA from control larvae groups as reference samples, and set to one. *Sox9a, sex determining region Y-box 9a*; *runx2, runt-related transcription factor 2*; *osx, osterix*; *col2a1a, collagen type 2 alpha 1a*; *grp1, gla-rich protein 1*; *alp, alkaline phosphatase*.

Finally, since not enough larvae from W125 group in the embryonic exposure trial survived until 16 dpf, gene expression was only evaluated in larvae from Control and W125 groups in the endotrophic exposure at the end of the trial (Fig. 4.21). In this case, *runx2* and *osx* gene expression was higher in W125 larvae compared to that of Control group larvae (one-way ANOVA, $P < 0.05$). In contrast, *col2a1a*, *mgp, bgp* and *alp* were not significantly affected by warfarin exposure (*t*-test, $P > 0.05$).

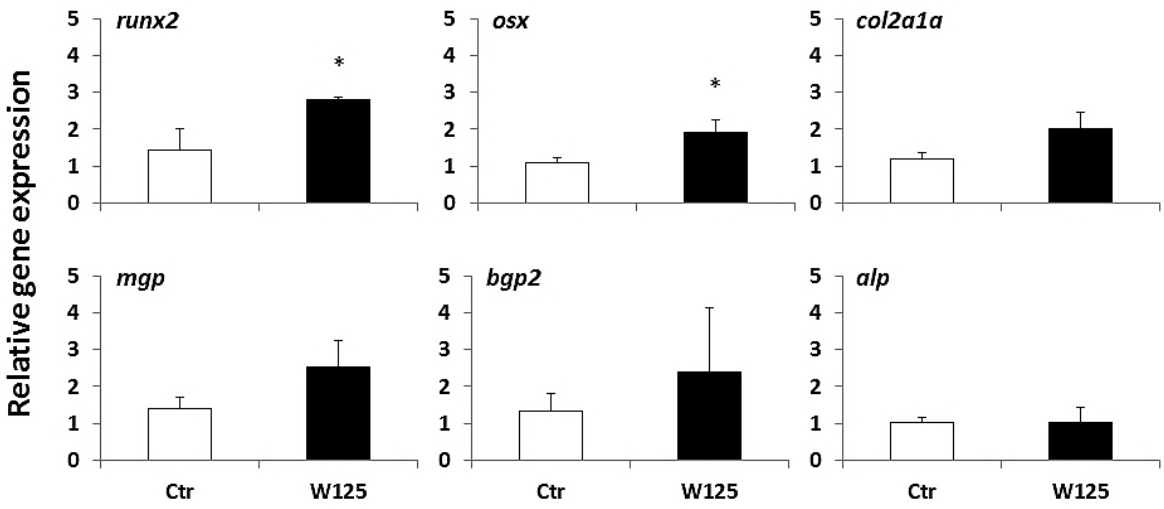

Figure 4.21. Relative expression of *runt-related transcription factor 2*, *osxterix*, *collagen type 2*, *matrix gla protein*, *bone gla protein* and *alkaline phosphatase* in zebrafish larvae at 16 dpf upon exposure to warfarin during larval stage: 0 (Ctr) and 125 (W125) mg L^{-1}. Transcript levels were determined by qPCR from 3 biological replicates (3 technical replicates per biological replicate) and normalized using *Rps18* housekeeping gene. An asterisk over the expression level of W125 group denotes statistical difference with the expression level of Control group (t-test; $P < 0.05$). Relative gene expression was determined using cDNA from control larvae groups as reference samples, and set to one. *Runx2, runt-related transcription factor 2*; *osx, osterix*; *col2a1a, collagen type 2 alpha 1a*; *mgp, matrix gla protein*; *bgp2, bone gla protein 2*; *alp, alkaline phosphatase*.

Chapter 5
Discussion

5. Discussion

It is known that warfarin can prevent VK action since it is responsible for the blockage of its recycling; and thus the blood coagulation by limiting the γ-carboxylation of coagulation factors (Stafford, 2005; Oldenburg et al., 2008). However, some undesired effect can arise when warfarin therapies are applied in humans. An example is the syndrome named Warfarin Embryopathy (WE), which comprises a wide range of manifestations like dysmorphology in neonate with *chondrodysplasia punctate* (nasal hypoplasia and stippling of epiphyses) and spine abnormalities (Menger et al., 1997; Sathienkijkanchai and Wasant, 2005; Mehndiratta et al., 2010) when pregnant women are under warfarin therapy.Some works have reported the teratogenic effects of warfarin exposure, like bleeding (Fernandez et al., 2014) and skeletal disorders (Weigt et al., 2012; Fernandez et al., 2014) using zebrafish as a model; however the main underlying pathways by which warfarin exposure during early development induce abnormal skeletogenesis are not known.

In this work we analyzed the effects of warfarin exposure during the early development of zebrafish, and new insights on the specific underlying mechanisms of abnormal skeletogenesis are provided.

Zebrafish larval performance under warfarin exposure

Warfarin exposure during the early development of zebrafish (embryonic and endotrophic stages) showed a set of negative effects on larval performance including growth retardation, hemorrhages, swimbladder underdevelopment, pericardiac inflammation, abnormal appearance of yolk sac, skeletogenesis disruption and increased mortality.

A major effect of warfarin exposure has been largely described in the literature: the blockage of VK recycling, through warfarin binding to vitamin K epoxide reductases (Vkor), which is needed as a cofactor for γ-glutamyl carboxylase (Ggcx) in order to perform the γ-carboxylation of VK dependent proteins (VKDPs; Stafford, 2005; Oldenburg et al., 2008) but also as a ligand for Pxr (Tabb et al., 2003). The γ-carboxylation is required to provide calcium binding properties to VKDPs (Stafford, 2005; Oldenburg et al., 2008) and thus, allowing them to control Ca^{2+} homeostais. Pxr plays important roles related to detoxification of the organism (drug metabolism), bone homeostasis, but also

regulating metabolic pathways for the elimination of cholesterol and regulating the glucose metabolism (Timsit and Negishi, 2007).

Growth retardation was found in larvae exposed to highest concentrations of warfarin, in particular to 125 mg L^{-1} exposure during embryonic as well as endotrophic stages. This feature is reported in literature (Menger et al., 1997; Hou, 2004), being present in infants exposed to warfarin during pregnancy (WE). Low standard length could be in a first moment explained by the effect promoted by warfarin in endochondral bone formation. Further, it also could be related in a second moment to malnutrition due to malformations in the mouth but also problems in locomotion, implying a lower success in catching live prey. As a consequence, this lower growth in larvae might affect survival, and explaining at least in part the higher mortality recorded in these larvae.

In larvae exposed to high concentrations of warfarin, hemorrhagic events were observed in brain as well as in abdominal region. The bleeding disorder have been already reported as an output of warfarin exposure in early development (Fernandez et al., 2014) and could be related to several factors; (i) decrease in γ-carboxylation of clotting factors, which are responsible for blood coagulation (Stafford, 2005; Oldenburg et al., 2008); (ii) ectopic calcification of soft tissues, in particular vascular tissues, due to the the undercarboxylated state of particular VKDPs like the Mgp (Schurgers et al., 2013). Mgp is synthesized by the vascular smooth muscle cells and is a major inhibitor of arterial calcification. Thus, its undercarboxylation promotes a reduction in the elasticity of the vessels (Luo et al., 1997). Bleeding disorders are one feature of WE in infants (Hou, 2004; Wainwright and Beighton, 2010; Mehndiratta et al., 2010). Further, Johnson et al. (2006) showed in Rambouillet sheep that defective γ-glutamyl carboxylase activity caused bleeding disorder in lambs, while brain bleeding disorder was observed by Spohn et al. (2009) in Vkorc1 knockout mice. Also Zhu et al. (2007) reported fatal hemorrhages in mice lacking γ -glutamyl carboxylase. More recently, Azuma et al. (2014) showed that γ-glutamyl carboxylase-deficient mice displayed bleeding due to the decreased activity of these coagulation factors. Bleeding disorder in zebrafish larvae exposed to warfarin, might be due to this already suggested pathways (uncarboxylated VKDPs). In this sense, present result are in agreement with the reported bleeding events when warfarin therapies were applied to pregnant women and being more severe during the earliest developmental stages of the fetus (Hou, 2004).

Larvae exposed to high concentrations of warfarin showed a more opaque yolk sac, for which the causative mechanisms are still unknown. Since yolk sac, majorly a store of lipids, is the nutritional resource of the larvae until its exotrophic stage, the opaque appearance of it might be related somehow with the reported role of Pxr in the control of lipid metabolism, regulating the transcription of several enzymes involved in lipid synthesis (Moreau et al., 2007; Sui et al., 2011; Bitter et al., 2014).

Regarding the pericardial inflammation under warfarin exposure, heart defects are reported in literature as an effect due to warfarin exposition, being a feature presented by infants carrying the WE (Hou, 2004). The cause of this pericardial inflammation is unknown, but could be related to the carboxylation state of different VKDPs already found to be expressed in heart (e.g. Mgp and growth-arrest specific 6 (Gas6)). Nevertheless, the inflammation present in pericardium might also account for the high mortality registered in these larvae.

In addition to the already reported effects of warfarin exposure during early development in vertebrates, treated larvae also showed an underdevelopment of the swimbladder. Warfarin was associated with respiratory problems and chronic lung disease (Hou, 2004) which might also due to the undercarboxylation of different VKDPs. According to Laurance et al. (2012), the Gas6 protein, another VKDP, seems to be involved in the functional activation of vascular smooth cells and endothelial cells, which are structural cells present in blood vessels. Since Gas6 needs to be γ-carboxylated in order to be biologically functional, an uncarboxylation of Gas6 under warfarin exposure would affect the formation of the blood vessels. Interestingly, fish swimbladder development and inflation is tightly controlled by a complex capillary net, called *rete mirabile* (Smith and Croll, 2012). Thus, an abnormal development of the swimbladder in fish exposed to warfarin might be due to the abnormal development/action of this *rete mirabile* under Gas6 uncarboxylation state. Mgp is also involved in vascular smooth cells homeostasis and particularly preventing its ectopic calcification (Schurgers et al., 2013), and its carboxylation state might be also altered in zebrafish exposed to warfarin. In addition to Gas6 and Mgp, another VKDP, Grp might be involved in an altered vascular development. Grp was defined as an inhibitor of vascular and valvular calcification, being involved in calcium homeostasis (Viegas et al., 2015). The same authors also reported that Grp function can be related to the prevention of calcium-induced signaling pathways and direct mineral binding to inhibit crystal formation and maturation. Nevertheless, additional

immunohistochemical and histological characterization of the vascular smooth cells, and particularly of the *rete mirabile*, are needed to address this issue.

Zebrafish skeletogenesis under warfarin exposure and underlying pathways

In this work we gave special emphasis on how an iduced VK deficiency by warfarin exposure during early development affects vertebrate's skeletogenesis. Previous works in fish species reported that VK is important to bone formation and homeostasis, being reported that a dietary VK deficiency induce a decrease in bone mineralization, leading to an increase of deformities in bone (Roy and Lall, 2007). Further, Richard et al. (2014) demonstrated that VK dietary supplementation during early development improve bone development in Senegalese sole (*Solea senegalensis*). Opposed approach applied in zebrafish demonstrated that warfarin treatment caused the disruption of skeletogenesis through Pxr signaling pathway and γ-glutamyl carboxylation of VKDPs (Fernandez et al., 2014).

From studies in mammals, there is increasing evidence that VK also positively affects calcium balance (Weber, 2001). *In vitro* studies showed that while VK_2 is a transcriptional regulator of bone marker genes in osteoblastic cells by activating the steroid and xenobiotic receptor (Sxr; Ichikawa et al., 2006); different VK metabolites promoted mineralization on human osteoblasts (Atkins et al., 2009).

The present research work showed that skeletal development in zebrafish larvae has been affected when they were exposed to high levels of warfarin (25 and 125 mg L^{-1}) during early developmental stages. Shorter bones, in particular endochondral bones, but also lower mineralization degree in endochondral and intramembranous bones have been reported. The observed effects are in agreement (at least partially) with the effects previously reported using knockout and *in vitro* systems. Shorter endochondral bones in zebrafish exposed to warfarin is in agreement with shorter long bones found in the mice lacking Vkorc1 (Spohn et al., 2009), while lower mineralization degree is in accordance with the reported lower osteoblast differentiation of osteoblastic cells treated with warfarin (Jeong et al., 2011). The main underlying pathways of this abnormal skeletogenesis seem to be related with the already proposed roles of VK: as a co-factor of Ggcx in γ-

carboxylation reaction of VKDPs (Oldenburg et al., 2008; Spohn et al., 2009) and Pxr signaling activation (Ichikawa et al., 2006; Azuma et al., 2010).

To unveil the possible skeletal specific pathways responsible for such abnormal skeletal development in zebrafish under warfarin exposure during early development, a gene specific expression analysis was performed. In this sense, expression of particular transcription factors (*sox9a, runx2, osx*), enzymes responsible of tissue mineralization (*alp*), but also proteins present in cartilage and bone extracellular matrix (*col2a1a, grp1, mgp,* and *bgp*) was evaluated at different sampling time points.

Sox9a, a key TF for the commitment of osteochondroprogenitor cells, chondrogenic mesenchymal condensation and proper chondrocyte proliferation, differentiation, maturation and hypertrophic conversion (Akiyama, 2008), was found to be down-regulated at 3 dpf in larvae exposed to the highest level of warfarin during embryonic stage. The lower length in endochondral structures found at 5 and 7 dpf larvae exposed to high warfarin doses is in agreement with the altered commitment of osteochondroprogenitor, chondrogenic mesenchymal condensation, chondrocyte proliferation, differentiation and/or maturation suggested by the *sox9a* down-regulation. Altered chondrogenesis might be finally translated in a reduced growth of cartilage in endochondral structures such as meckel's cartilage, ceratohyal and ceratobranchial arches and the ethmoid plate. In fact, abnormal endochondral structures development under this specific pathway has been previously reported as a cause of perinatal death in *Sox9* heterozygous mutant mice (Bi et al., 2001), with cleft palate, as well as hypoplasia and bending of many skeletal structures derived from cartilage precursors. Furthermore, mutations in one allele of *Sox9* in humans result in campomelic dysplasia (CD), a skeletal dysplasia characterized by sex reversal and skeletal malformations of endochondral bones (Mori-Akiyama et al., 2003). This is the first work reporting an altered gene expression of *sox9a* under warfarin exposure as the potential underlying pathway of abnormal chondrogenesis.

Another critical TF in skeletal development analyzed was *runx2.* Runx2 is essential in the terminal differentiation of chondrocytes, a prerequisite for endochondral ossification. Also, during osteoblast differentiation, it plays essential roles in the commitment of pluripotent mesenchymal cells to the osteoblastic lineage (reviewed in Komori, 2010). Mundlos et al., (1997) demonstrated that mutations in r*unx2* are responsible to produce skeletal defects (such as hypoplastic clavicles, open fontanelles, Wormian bones and hypoplastic scapulae) in mice, similar to those found in human Cleidocranial dysplasia

(CCD; disorder that affect endochondral and intramembranous bone formation). Komori et al. (1997) showed that the disruption of *runx2* results in a complete lack of bone formation due to maturational arrest of osteoblasts. *Runx2* knockout mice showed dwarfism and had short legs, exhibiting also a deficit in mineralization. Interestingly, the effects on skeletal development under an induced VK deficiency during early development (5 and 7 dpf) do not seem to be due to an altered runx2 signaling pathway, as suggest by the gene expression analysis.

The last TF important in skeletal development analyzed was *osx*. Osx is a major effector and essential for osteoblast differentiation, activating bone-specific genes that support bone formation (reviewed in Shina and Zhou, 2013). Zhou et al. (2010) reported that the inactivation of *osx* in mice after birth causes multiple skeletal phenotypes including lack of new bone formation, absence of resorption of mineralized cartilage, and defects in osteocyte maturation and function. Also, Ren and Winkler (2014) showed that *osx* ablation led to a delay of osteoblast maturation in early bone structures resulting in smaller and malformed structures in medaka (*Oryzas latipes*). Further, recently Huang and Olsen (2015) have reported that a conditional knockdown of *osx* in mice have induced skeletal deformities, including delayed calvarial ossification.

In larvae exposed to high doses of warfarin during embryonic stage no significant differences were found at 3 dpf, in agreement with the minimal population of osteoblast cells found at this developmental stage. However, in larvae at 5 dpf exposed to warfarin during the endotrophic stage, *osx* was found significantly down-regulated compare with Control larvae. This results are in agreement with the reported lower mineralization in patients with a frameshift mutation in *osx* (Lapunzina et al., 2010) and the reported inhibition of osteoblastic differentiation by warfarin exposure and the *osx* down-regulation in those cells (Jeong et al., 2011). A lower expression of *osx* in zebrafish larvae during endotrophic stage is in accordance with previous reports about the key role of Osx in osteoblastogenesis, and coherent with the reported lower mineralization degree in endochondral and intramembranous structures in those warfarin exposed larvae. Thus, present result suggest that abnormal skeletal development in larvae exposed to warfarin might be due to an altered osteoblastogenesis through *osx* pathway and not due to altered *runx2* signaling.

Surprisingly, larvae exposed to warfarin during early development showed late effects on its skeletogenesis, being found a high percentage of larvae treated with highest

concentration of warfarin with a lower mineralization degree of vertebral bodies. Although it was not possible to evaluate the gene expression of TF in larvae from W125 group from the embryonic trial at 16 dpf, the analysis of the same group from endotrophic trial showed an up-regulation of *osx* and *runx2*. Those results are consistent with the delayed osteoblastogenesis process in those larvae compared with larvae from the Control group, where cartilage and bone cells were still in differentiation and both TFs are expressed.

Further demonstration that chondrogenesis and osteoblastogenesis were impaired in zebrafish larvae exposed to warfarin during early developmental stages was made by analyzing the expression of other skeletal development marker genes. In this sense, *tissue-nonspecific alkaline phosphatase* (*tnap;* and from now on *alp*) gene expression analysis showed that it was only found significantly down-regulated at 5 dpf in larvae exposed to highest levels of warfarin during endotrophic stages. *Alp* is normally induced during the early stage of osteoblastogenesis and participates in collagen calcification during bone formation (Millan, 2013). Mutations in *alp* caused inadequate or defective mineralization of the skeleton (in particular, hypophosphatasia), caused by an arrest in the propagation of hydroxyapatite crystals onto the collagenous ECM (reviewed in Millan, 2013). Furthermore, Liu et al. (2014) recently showed that *alp* knockout caused abnormal craniofacial bone development, with mice exhibiting a severely diminished bone mineralization. Taking this into account, present results of lower gene expression of *alp* at 5 dpf is in agreement and consistent with the down-regulation of *osx* in the same larvae as well as the lower mineralization degree on endochondral and intramembranous structures.

Genes encoding ECM proteins were also found to be differentially expressed. Col2a1a is expressed by chondrocytes and the main structural component of cartilage, providing to it shock absorbing properties and resistance to stress (Gelse et al., 2003). It has been suggested that the expression of the *type 2 collagen* gene may define and determine the sites and timing of chondrogenesis (Thorogood et al., 1986). Vandenberg et al., (1991) has reported that expression of a partially deleted human *type 2 procollagen* (*col2a1*) gene in transgenic mice produced a chondrodysplasia characterized by a range of features including short and thick limbs, and delayed mineralization of bone. Same feature (lower mineralization degree and short bones) have been observed in our warfarin-treated larvae, where a down-regulation of *col2a1a* was also found at 3 dpf in larvae exposed during embryonic stages as well as a negative correlation with warfarin concentration in larvae from the endotrophic strage trial at 5 dpf. Furthermore, such down-regulation is

consistent with the one observed in *sox9a* in 3 dpf larvae from the embryonic trial and the reported lack of expression of chondrocyte-specific markers, such as *col2a1*, *col2a2*, and *aggrecan* in mouse embryo chimeras derived from *Sox9* $^{-/-}$ embryonic stem cells (Bi et al., 1999).

Grp1 gene expression was also analyzed at 3 and 5 dpf during embryonic and endotrophic trials, respectively. *Grp* has been reported to be expressed in several skeletal cell types including chondrocytes, osteocytes and osteoblasts, with chondrocytes being the major site of expression (reviewed in Cancela et al., 2012). Further, it was identified in the calcified cartilage of *Adriatic sturgeon* (Viegas et al., 2008), and therefore a role in cartilage development was initially suggested. More recently, Grp was defined as an inhibitor of vascular and valvular calcification, being involved in calcium homeostasis (Viegas et al., 2015) as other VKDPs. Viegas et al. (2015) also reported that Grp function can be related to the prevention of calcium-induced signaling pathways and direct mineral binding to inhibit crystal formation and maturation. In zebrafish, two *grp* isoforms (*grp1* and *grp2*) have been identified (Fazenda et al., 2012). *Grp* expression appear to be inversely correlated, being *grp1* expressed first and remaining high during early development. In contrast, expression of *grp2* appears later and increases in late larval and juvenile stages, having greater prevalence in adult tissues (Fazenda et al., 2012). In our analysis, *grp1* was found to be down-regulated at 3 and 5 dpf, concomitant with the reduced chondrogenesis and osteoblastogenesis identified by double staining and supported by gene expression of *sox9a* and *col2a1a*.

Finally, two VKDP's important in skeletal development, Mgp and Bgp, were also analyzed at 16 dpf in Control and W125 groups from endotrophic trial. Mgp, expressed in several tissues and synthesized predominantly by chondrocytes has as principal function limiting calcification in soft tissues (reviewed in Schurgers et al., 2013). In mammals this protein has been associated with the differentiation and maturation of chondrocytes being a key regulator of fish endochondral and intramembranous ossification. Mice lacking Mgp developed arterial calcification which leads to blood vessel rupture, and exhibited inappropriate calcification of various cartilages, including the growth plate, which eventually led to short stature, osteopenia and fractures (Luo et al., 1997). Humans that lack functional Mgp showed calcification of cartilage but did not exhibit the gross vascular calcification observed in mice (Munroe et al., 1999). Regarding Bgp, in several teleosts, including zebrafish, two *bgp* isoforms (*bgp1* and *bgp2*) have been identified (Laizé et al.,

2006). *Bgp1* is detected in the notochord sheath during chordacentrum formation, whereas *bgp2* is only expressed later in association with bone formation (Bensimon-Brito et al., 2012). *Bgp* is generally expressed by mature and resting osteoblasts and by hypertrophic chondrocytes (Bensimon-Brito et al., 2012), being suggested that is required to stimulate bone mineral maturation (Boskey et al., 1998). Although Pinto et al. (2001) suggested that Bgp in fish is associated with bone mineralization and Kavukcuoglu et al. (2009) suggested that this protein plays an important role in the growth of apatite crystals in bone by increasing the degree of carbonate substitutions; Karsenty and Ferron (2012) recently described Bgp as a VKDP with a broader physiological roles in the whole organism. Mice deficient in the *osteocalcin* (or *bgp*) gene suggested a coordinated regulation of bone mass or growth, energy metabolism and reproduction (reviewed in Karsenty and Ferron, 2012). Previous works in our lab found that while an induced VK deficiency affected *mgp* and *bgp1* expression in zebrafish larvae (both of them were found up-regulated; Fernandez et al., 2014); *bgp1* was found down-regulated in fish fed VK supplemented diets (Richard et al., 2014). In this work, *mgp* as *bgp2* were not differentially expressed at 16 dpf in Control and W125 larvae. This could be due to the fact that in zebrafish, both *bgp* and *mgp* mRNAs are expressed in skeletal tissues before, during and after mineralization (Gavaia et al., 2006).

Chapter 6
Conclusions

6. Conclusions

This study showed that VK deficiency induced by warfarin exposure during short time at critical early (embryonic and endotrophic) developmental stages has a great impact on zebrafish development, causing growth retardation, hemorrhages, swimbladder underdevelopment, pericardiac inflammation, opaque appearance of yolk sac, skeletogenesis disruption and increase on mortality. Warfarin exposure effects were found developmental stage and dose dependent, being larvae exposed to 125 mg L^{-1} of warfarin during embryonic stage mimicking WE. Although these effects might be directly related to the impairment of VK status and the consequent decrease of the γ-carboxylation of different VKDPs and the lower activation of Pxr signaling pathway; new insights on the particular biological process (chondrogenesis and osteoblastogenesis) and their underlying signaling pathway (altered expression of *sox9a* and *osx*) were reported. Further, this study demonstrated that zebrafish is a suitable model for understanding the differential effects of VK deficiency when it occurs at early life stages, allowing to identify potential underlying mechanisms of WE, and not only regarding the abnormal bone formation.

Chapter 7
Future perspectives

7. Future perspectives

Our work suggested some possible pathways affected by a VK deficiency. In this sense, further confirmation might be done by the use of transgenic lines, in particular those expressing genes associated with chondrogenesis (*sox9a*) or osteoblastogenesis (*osx*) to analyze *in vivo* the effects promoted by this VK deficiency. In addition, *in situ hybridization* procedures might give some light on the specific cell types and state (proliferating and/or differentiating chondrocytes and osteoblast) where abnormal expression of *sox9a* and *osx* took place; or western blot and inmmunohistochemistry with their specific antibodies for confirming abnormal gene expression has been translated in altered protein synthesis and/or VKDPs γ-carboxylation state. Further, since our results suggested that other complications are related to a deficiency in VK, it would be interesting to analyze the effects caused by it in the vascular tissue, brain and eyes development but also in other vital structures, such as the heart, through histological procedures.

Finally, a wider transcriptomic analysis of larvae exposed to warfarin might give new insights on different biological process further affected by induced VK deficiency; while a Chip-seq analysis could identify the specific targeted genes by warfarin exposure under Pxr signaling.

Chapter 8
References

8. References

Akiyama H., 2008. Control of chondrogenesis by the transcription factor Sox9. Modern Rheumatology, 18: 213-219

Andersen, C. L., Jensen, J. L., Ørntoft, T. F., 2004. Normalization of real-time quantitative reverse transcription-PCR data: a model-based variance estimation approach to identify genes suited for normalization, applied to bladder and colon cancer data sets. Cancer Research, 64: 5245-5250

Atkins J. G., Welldon J. K., Wijenayaka R. A., Bonewald F. L., Findlay M. D., 2009. Vitamin K promotes mineralization, osteoblast-to-osteocyte transition, and an anticatabolic phenotype by γ-carboxylation-dependent and -independent mechanisms. American Journal of Physiology - Cell Physiology, 297: C1358-C1367

Azuma K., Casey C. S., Ito M., Urano T., Horie K., Ouchi Y., Kirchner S., Blumberg B., Inoue S., 2010. Pregnane X receptor knockout mice display osteopenia with reduced bone formation and enhanced bone resorption. Journal of Endocrinology 207: 257-263

Azuma K., Tsukui T., Ikeda K., Shiba S., Nakagawa K., Okano T., Urano T., Horie-Inoue K., Ouchi Y., Ikawa M., Inoue S., 2014. Liver-specific γ-glutamyl carboxylase-deficient mice display bleeding diathesis and short life span. PLoS ONE, 9: e88643

Baek W., Lee M., Jung W. J., Kim S., Akiyama H., de Crombrugghe B., Kim J., 2009. Positive regulation of adult bone formation by osteoblast-specific transcription factor Osterix. Journal of Bone and Mineral Research, 24: 1055-1065

Beinema M., Brouwers J.R.B.J., Schalekamp T., Wilffert B., 2008. Pharmacogenetic differences between warfarin, acenocoumarol and phenprocoumon. Thrombosis and Haemostasis, 100: 1052-1057

Bensimon-Brito A., Cardeira J., Cancela L. M., Huysseune A. Witten E. P., 2012. Distinct patterns of notochord mineralization in zebrafish coincide with the localization of Osteocalcin isoform 1 during early vertebral centra formation. BMC Developmental Biology. 12: 28

Bi W., Deng M. J., Zhang Z., Behringer R. R., de Crombrugghe B., 1999. Sox9 is required for cartilage formation. Nature Genetics, 22: 85-89

Bi W., Huang W., Whitworth J. D., Deng M. J., Zhang Z., Behringer R. R., de Crombrugghe B., 2001. Haploinsufficiency of Sox9 results in defective cartilage primordia and premature skeletal mineralization. Proceedings of the National Academy of Sciences of the United States of America, 98: 6698-6703

Bird C. N. and Mabee M. P., 2014. Developmental morphology of the axial skeleton of the zebrafish, danio rerio (ostariophysi: cyprinidae). Developmental Dynamics 228: 337–357, 2003

Bitter A., Rümmele P., Klein K., Kandel A. B., Rieger K. J., Nüssler K. A., Zanger M. U., Trauner M., Schwab M., Burk O., 2014. Pregnane X receptor activation and silencing promote steatosis of human hepatic cells by distinct lipogenic mechanisms. Archives of Toxicology. 1-15

Boskey L. A., Gadaleta S., Gundberg C., Doty B. S., Ducy P. , Karsenty G., 1998. Fourier transform infrared microspectroscopic analysis of bones of osteocalcin-deficient mice provides insight into the function of osteocalcin. Bone, 23: 187-196

Boyle J. W., Simonet S. W., Lacey L. D., 2003. Osteoclast differentiation and activation. Nature, 423: 337-342

Cancela L. M., Conceição N.,and Laizé V., 2012. Gla-rich protein, a new player in tissue calcification?. Advances in Nutrition, 3: 174–181

Chang J., Wang Z., Tang E., Fan Z., McCauley L., Franceschi R., Guan K., Krebsbach H. P., Wang Y. C., 2009. Inhibition of osteoblastic bone formation by nuclear factor-kB. Nature Medicine, 15: 682-689

de Crombrugghe B., Lefebvre V., Nakashima K., 2001. Regulatory mechanisms in the pathways of cartilage and bone formation. Current Opinion in Cell Biology, 13:721-727

Derveaux S., Vandesompele J., Hellemans J., 2010. How to do successful gene expression analysis using real-time PCR. Methods, 50: 227-230

Ekins S., Reschly J. E., Hagey R. L., Krasowski, D. M., 2008. Evolution of pharmacologic specificity in the pregnane X receptor. BMC Evolutionary Biology, 8: 103

Fazenda C., Silva L. A. I., Cancela L. M., Conceição N., 2012. Molecular characterization of two paralog genes encoding Gla-rich protein (Grp) in zebrafish. Journal of Applied Ichthyology, 28: 377-381

Ferland, G., 2012. Vitamin K and the nervous system: an overview of its actions. Advances in Nutrition, 3: 204-212

Fernández I., Santos A., Cancela L. M., Laizé V., Gavaia J. P., 2014. Warfarin, a potential pollutant in aquatic environment acting through Pxr signaling pathway and γ-glutamyl carboxylation of vitamin K-dependent proteins. Environmental Pollution, 194: 86-95

Fernández I., Vijayakumar P., Marques C., Cancela L. M., Gavaia J. P., Laizé V., 2015. Zebrafish vitamin K epoxide reductases: expression in vivo, along extracellular matrix mineralization and under phylloquinone and warfarin in vitro exposure. Fish Physiology and Biochemistry, 41: 745-759

Franz-Odendaal A. T., Hall K. B., Witten E. P., 2006. Buried Alive: How Osteoblasts Become Osteocytes. Developmental Dynamics, 235: 176-190

Gavaia J. P., Simes C. D., Ortiz-Delgado J.B., Viegas B. S. C., Pinto P. J., Kelsh N. R., Sarasquete C. M., Cancela M. L., 2006. Osteocalcin and matrix Gla protein in zebrafish (Danio rerio) and Senegal sole (Solea senegalensis): Comparative gene and protein expression during larval development through adulthood. Gene Expression Patterns 6: 637–652

Gelse K., Poschl E., Aigner T., 2003. Collagens—structure, function, and biosynthesis. Advanced Drug Delivery Reviews, 55: 1531-1546

Gérard Karsenty and Mathieu Ferron. The contribution of bone to whole-organism physiology. Nature, 481: 314–320, 2012

Gómez-Outes A., Lecumberri R., Pozo C. Rocha E., 2009. New Anticoagulants: Focus on Venous Thromboembolism. Current Vascular Pharmacology, 7: 309-329

Gómez-Outes A., Suárez-Gea L. M., Lecumberri R., Terleira-Fernández I. A., Vargas-Castrillón E., Rocha E., 2013. Potential role of new anticoagulants for prevention and treatment of venous thromboembolism in cancer patients. Vascular Health and Risk Management, 9: 207-228

Greer R. F., 2010. Vitamin K the basics—What's new?. Early Human Development, 86: S43-S47

Gu X., Ke S., Liu D., Sheng T., Thomas P. E., Rabson A. B., Gallo M. A., Xie W., Tian Y., 2006. Role of NF-kB in regulation of PXR-mediated gene expression: a mechanism for the suppression of cytochrome P-450 3A4 by proinflammatory agents. Journal of Biological Chemistry, 281: 17882-17889

Hall G. J., Pauli M. R., Wilson M. K., 1980. Maternal and fetal sequelae of anticoagulation during pregnancy. The American Journal of Medicine, 68: 122-40

HALL, K. B.; Bones and Cartilage: Developmental and Evolutionary Skeletal Biology, Second Edition. London. Elsevier Press, 2015. 978-0-12-416678-3

Hammed A., Matagrin B., Spohn G., Prouillac C., Benoit E., Lattard V., 2013. VKORC1L1, an enzyme rescuing the vitamin K 2,3-epoxide reductase activity in some extrahepatic tissues during anticoagulation therapy. The Journal of Biological Chemistry, 288: 28733-28742

Hanumanthaiah R., Thankavel B., Day K., Gregory M., Jagadeeswaran P., 2001. Developmental expression of vitamin K-dependent gamma-carboxylase activity in zebrafish embryos: effect of warfarin. Blood Cells, Molecules and Diseases, 27: 992-999

Hou J., 2004. Fetal Warfarin Syndrome. Chang Gung Medical Journal, 27: 691-695

Huang P., Chandra V., Rastinejad F., 2010. Structural overview of the nuclear receptor superfamily: insights into physiology and therapeutics. Annual Review of Physiology, 72: 247-272

Huang W., Olsen R. B., 2015. Skeletal defects in Osterix-Cre transgenic mice. Transgenic Research, 24: 167-172

Ichikawa T., Horie-Inoue K., Ikeda K., Blumberg B., Inoue S., 2006. Steroid and xenobiotic receptor SXR mediates vitamin K2-activated transcription of extracellular matrix-related genes and collagen accumulation in osteoblastic cells. The Journal of Biological Chemistry, 281: 16927-16934

Jeong H.M., Cho D.H., Jin Y.H., Chung J.O., Chung M.N., Chung D.J., Lee K.Y., 2011. Inhibition of osteoblastic differentiation by warfarin and 18-α-glycyrrhetinic acid. Archives of Pharmaceutical Research, 34: 1381-1387

Jiang X., Ye M., Jiang X., Liu G., Feng S., Cui L., Zou H., 2007. Method development of efficient protein extraction in bone tissue for proteome analysis. Journal of Proteome Research, 6: 2287-2294

Jimi E., Aoki K., Saito H., D'Acquisto F., May J. M., Nakamura I., Sudo T., Kojima T., Okamoto F., Fukushima H., Okabe K., Ohya K., Ghosh S., 2004. Selective inhibition of NF-kB blocks osteoclastogenesis and prevents inflammatory bone destruction in vivo. Nature Medicine, 10: 617-624.

Johnson S. J., Soute A. B., Olver S. C., Baker C. D., 2006. Defective c-Glutamyl Carboxylase Activity and Bleeding in Rambouillet Sheep. Veterinary Pathology, 43: 726-732

Kamali F., Wynne H., 2010. Pharmacogenetics of Warfarin. Annual Review of Medicine, 61: 63-75

Karsenty G., 2008. Transcriptional Control of Skeletogenesis. The Annual Review of Genomics and Human Genetics, 9: 183-96

Kavukcuoglu B. N., Patterson-Buckendahl P., Manna B. A., 2009. Effect of osteocalcin deficiency on the nanomechanics and chemistry of mouse bones. Journal of the Mechanical Behavior of Biomedical Materials, 2: 348 -354

Kohli P., Cannon P. C., 2013. Dabigatran associated with increased risk of acute coronary events. Evidence-Based Medicine, 18: e9

Komori T., 2010. Regulation of bone development and extracellular matrix protein genes by Runx2. Cell and Tissue Research, 339: 189-195

Komori T., Yagi H., Nomura S., Yamaguchi A., Sasaki K., Deguchi K., Shimizu Y., Bronson T. R., Gao H. Y., Inada M., Sato M., Okamoto R., Kitamura Y., Yoshiki S., Kishimoto T., 1997. Targeted disruption of Cbfa1 results in a complete lack of bone formation owing to maturational arrest of osteoblasts. Cell, 89: 755-764

Kuruvilla M., Gurk-Turner C., 2001. A review of warfarin dosing and monitoring. BUMC Proceedings, 14: 305-306

Laizé V., Viegas B. S. C., Price A. P., Cancela L. M., 2006. Identification of an Osteocalcin isoform in fish with a large acidic prodomain. The Journal of Biological Chemistry, 281: 15037-15043

Lapunzina P., Aglan M., Temtamy S., Caparrós-Martín A. J., Valencia M., Letón R., Martínez-Glez V., Elhossini R., Amr K., Vilaboa N., Ruiz-Perez L. V., 2010. Identification of a frameshift mutation in Osterix in a patient with recessive Osteogenesis Imperfecta. The American Journal of Human Genetics, 87: 110-114

Latchman S. D., 1997. Transcription factors: an overview. The International Journal of Biochemistry and Cell Biology, 29: 1305-1312

Laurance S., Lemarie A.C., Blostein D.M., 2012. Growth arrest-specific gene 6 (Gas6) and vascular hemostasis. Advances in Nutrition, 3: 196-203

Lee I. T., Young A. R., 2000. Transcription of eukaryotic protein-coding genes. Annual Review of Genetics, 34: 77-137

Li J., Lin C. J., Wang H., Peterson W. J., Furie C. B., Furie B., Booth L. S., Volpe J. J., Rosenberg A. P., 2003. Novel role of vitamin K in preventing oxidative injury to developing oligodendrocytes and neurons. The Journal of Neuroscience, 23: 5816-5826

Lieschke J. G., Currie D. P., 2007. Animal models of human disease: zebrafish swim into view. Nature Reviews Genetics, 8: 353-367

Liu J., Nam K. H., Campbell C., Cristina da Silva Gasque K., Millán L. J., Hatch E. N., 2014. Tissue-nonspecific alkaline phosphatase deficiency causes abnormal craniofacial bone development in the $Alpl^{-/-}$ mouse model of infantile hypophosphatasia. Bone, 67: 81-94

Luo, G., Ducy P., McKee D. M., Pinero J. G., Loyer E., Behringer R. R., Karsenty G., 1997. Spontaneous calcification of arteries and cartilage in mice lacking matrix GLA protein. Nature 386: 78-81

Mehndiratta S., Suneja A., Gupta B. and Bhatt S., 2010. Fetotoxicity of warfarin anticoagulation. Archives of Gynecology and Obstetrics, 282: 335–337

Menger H., Lin A.E., Toriello H.V., Bernert G., Spranger J.W., 1997. Vitamin K deficiency embryopathy: a phenocopy of the warfarin embryopathy due to a disorder of embryonic vitamin K metabolism. American Journal of Medical Genetics, 72:129-134

Millán L. J., 2013. The role of phosphatases in the initiation of skeletal mineralization. Calcified Tissue Internationa, 93: 299-306

Moreau A., Maurel P., Vilarem J. M., Pascussi M. J., 2007. Constitutive androstane receptor–vitamin D receptor crosstalk: Consequence on CYP24 gene expression. Biochemical and Biophysical Research Communications, 360: 76-82

Mori-Akiyama Y., Akiyama H., Rowitch H. D., de Crombrugghe B., 2003. Sox9 is required for determination of the chondrogenic cell lineage in the cranial neural crest. Proceedings of the National Academy of Sciences of the United States of America, 100: 9360-9365

Moyer P. T., O'Kane J. D., Baudhuin M. L., Wiley L. C., Fortini A., Fisher K. P., Dupras M. D., Chaudhry R., Thapa P., Zinsmeister R. A., Heit A. J., 2009. Warfarin sensitivity genotyping:a review of the literature and summary of patient experience. Mayo Clinic Proceedings, 84: 1079-1094

Mukai K., Morimoto H., Kikuchi S., Nagaoka S., 1993. Kinetic study of free-radical-scavenging action of biological hydroquinones (reduced forms of ubiquinone, vitamin K and tocopherol quinone) in solution. Biochimica et Biophysica Acta, 1157: 313-317

Mundlos S., Otto F., Mundlos C., Mulliken B. J., Aylsworth S. A., Albright S., Lindhout D., Cole G. W., Henn W., Knoll M. H. J., Owen J. M., Mertelsmann R., Zabel U. B., Olsen R. B., 1997. Mutations involving the transcription factor Cbfa1 cause cleidocranial dysplasia. Cell, 89: 773-779

Munroe B. P., Olgunturk O. R., Fryns P. J., Van Maldergem L., Ziereisen F., Yuksel B., Gardiner M. R., Chung E., 1999. Mutations in the gene encoding the human matrix Gla protein cause Keutel syndrome. Nature Genetics, 21: 142 – 144

Myllyharju J., 2014. Extracellular matrix and developing growth plate. Current Osteoporosis Reports, 12: 439-445

Oldenburg J., Marinova M., Muller-Reible C. and Watzka M., 2008. The Vitamin K Cycle. Vitamins and Hormones, 78:35-62

Oldenburg J., Watzka M.. Bevans G. C., 2015. VKORC1 and VKORC1L1: Why do vertebrates have two Vitamin K 2,3-Epoxide Reductases?. Nutrients, 7: 6250-6280

Olsen R.B., Reginato M.A., Wang W., 2000. Bone development. Annual Review of Cell and Developmental Biology, 16: 191-220

Pelster B., 2004. pH regulation and swimbladder function in fish. Respiratory Physiology and Neurobiology, 144: 179-190

Pfaffl M.W., 2001. A new mathematical model for relative quantification in realtime RT-PCR. Nucleic Acids Research, 29: e45

Pfaffl M.W., Tichopad A., Prgomet C., Neuvians T.P., 2004. Determination of stable housekeeping genes, differentially regulated target genes and sample integrity: bestKeeper - Excel-based tool using pair-wise correlations. Biotechnology Letters, 26: 509-515

Pinto P. J., Ohresser P. C. M., Cancela L. M., 2001. Cloning of the bone Gla protein gene from the teleost fish Sparusaurata. Evidence for overall conservation in gene organization and bone-specific expression from fish to man. Gene, 270: 77–91

Renn J., Winkler C., 2014. Osterix/Sp7 regulates biomineralization of otoliths and bone in medaka (Oryzias latipes). Matrix Biology, 34: 193-204

Richard N., Fernández I., Wulff T., Hamre K., Cancela L. M., Conceição C. E. L., Gavaia J. P., 2014. Dietary supplementation with vitamin k affects transcriptome and proteome of senegalese sole, improving larval performance and quality. Marine Biotechnology 16: 522-537

Roy P. K., Lall P. S., 2007. Vitamin K deficiency inhibits mineralization and enhances deformity in vertebrae of haddock (Melanogrammus aeglefinus L.). Comparative Biochemistry and Physiology, 148B: 174-183

Sathienkijkanchai A., Wasant P., 2005. Fetal Warfarin Syndrome. Journal of the Medical Association of Thailand, 88: S246-250

Schurgers J. L., Uitto J., Reutelingsperger P. C., 2013. Vitamin K-dependent carboxylation of matrix Gla-protein: a crucial switch to control ectopic mineralization. Trends in Molecular Medicine, 19: 217-226

Shearer J. M., 2009. Vitamin K in Parenteral Nutrition. Gastroenterology, 137: 105-118

Shearer J. M., Newman P., 2014. Recent trends in the metabolism and cell biology of vitamin K with special reference to vitamin K cycling and MK-4 biosynthesis. The Journal of Lipid Research, 55: 345-362

Sinha M. K., Zhou X., 2013. Genetic and molecular control of Osterix in skeletal formation. Journal of Cellular Biochemistry, 114: 975-984

Sire Y.J., Donoghue C.P., Vickaryous K.M., 2009. Origin and evolution of the integumentary skeleton in non-tetrapod vertebrates. Journal of Anatomy, 214: 409-440

Smith M. F., Croll P. R., 2011. Autonomic control of the swimbladder. Autonomic Neuroscience: Basic and Clinical, 165: 140-148

Spohn G., Kleinridders A., Wunderlich F.T., Watzka M., Zaucke F., Blumbach K., Geisen C., Seifried E., Müller C., Paulsson M., Brüning J.C., Oldenburg J., 2009. VKORC1 deficiency in mice causes early postnatal lethality due to severe bleeding. Thrombosis and Haemostasis, 101: 1044-1050

Stafford W. D., 2005. The vitamin K cycle. Journal of Thrombosis and Haemostasis, 3: 1873-1878

Sui Y., Xu J., Rios-Pilier J., Zhou C., 2011. Deficiency of PXR decreases atherosclerosis in apoE-deficient mice. Journal of Lipid Research, 52: 1652-1659

Sutor H. A., von Kries R., Cornelissen A. E., McNinch W. A., Andrew M., 1999. Vitamin K Deficiency Bleeding (VKDB) in Infancy. Thrombosis and Haemostasis, 81: 456-61

Tabb M. M., Sun A., Zhou C., Grun F., Errandi J., Romero K., Pham H., Inoue S., Mallick S., Lin M., Forman M. B. and Blumberg B., 2003. Vitamin K2 Regulation of Bone Homeostasis Is Mediated by the Steroid and Xenobiotic Receptor SXR. J. Biol. Chem. 278: 43919-43927

Takada H., Toru H., Bunya, N., Kiriu, N., Kato, H., Koido, Y., Yasuhiro, K., 2014. Acquired absolute vitamin K deficiency in a patient undergoing warfarin therapy. American Journal of Emergency Medicine, 32: 688.e1-688.e2

Thorogood P., Bee J., von der Mark K., 1986. Transient expression of cartilage type IT at epitheliomesenchymal interfaces during morphogenesis of the cartilaginous neurocranium. Developmental Biology, 116: 497-509

Timsit E. Y., Negishi M., 2007. CAR and PXR: The Xenobiotic-Sensing Receptors. Steroids, 72: 231-246

Vandenberg P., Khillan S. J., Prockop J. D., Helminen H., Kontusaari S., Ala-Kokko L., 1991. Expression of a partially deleted gene of human type II procollagen (COL2A1) in transgenic mice produces a chondrodysplasia. Proceedings of the National Academy of Sciences of the United States of America, 88: 7640-7644

Viegas B. S. C., Simes C. D., Laizé V., Williamson K. M., Price A. P. and Cancela L. M., 2008. Gla-rich Protein (GRP), A New Vitamin K-dependent Protein Identified from Sturgeon Cartilage and Highly Conserved in Vertebrates. The Journal of Biological Chemistry, 283: 36655–36664

Viegas S. C., Rafael S. M., Enriquez L. J., Teixeira A., Vitorino R,, Luís M. I., Costa M. R., Santos S., Cavaco S., Neves J., Macedo L. A., Willems A. B., Vermeer C., Simes C. D., 2015. Gla-rich protein acts as a calcification inhibitor in the human cardiovascular system. Arteriosclerosis, Thrombosis, and Vascular Biology, 35: 399-408

Wainwright H., Beighton P., 2010. Warfarin embryopathy: fetal manifestations. Virchows Arch 457: 735-739

Wallace D. B., Betts L., Talmage G., Pollet M. R., Holman S. N., Redinbo R. M., 2013. Structural and functional analysis of the human nuclear xenobiotic receptor PXR in complex with RXRα. Journal of Molecular Biology, 425: 2561-2577

Walker B. M., Kimmel B. C., 2007. A two-color acid-free cartilage and bone stain for zebrafish larvae. Biotechnic and Histochemistry, 82: 23-28

Weber P., 2001. Vitamin K and bone health. Nutrition, 17: 880-887

Weigt S., Huebler N., Strecker R., Braunbeck T., Broschard T.H., 2012. Developmental effects of coumarin and the anticoagulant coumarin derivative warfarin on zebrafish (Danio rerio) embryos. Reproductive Toxicology, 33: 133-141

Westhofen P., Watzka M., Marinova M., 2011. Human vitamin K 2,3-epoxide reductase complex subunit 1-like 1 (VKORC1L1) mediates vitamin K-dependent intracellular antioxidant function. Journal of Biological Chemistry, 286: 15085-15094

Witten E. P., Hansen A., Hall K. B., 2001. Features of mono- and multinucleated bone resorbing cells of the zebrafish danio rerio and their contribution to skeletal development, remodeling, and growth. Journal of Morphology, 250:197-207

Witten E.P. and Huysseune A., 2009. A comparative view on mechanisms and functions of skeletal remodelling in teleost fish, with special emphasis on osteoclasts and their function. Biological reviews of the Cambridge Philosophical Society, 84: 315-46

Zhou C., Assem M., Tay C. J., Watkins B. P., Blumberg B., Schuetz G. E., Thummel E. K., 2006. Steroid and xenobiotic receptor and vitamin D receptor crosstalk mediates CYP24 expression and drug-induced osteomalacia. Journal of Clinical Investigation, 116: 1703-1712

Zhu A., Sun H., Raymond M. R., Furie C. B., Furie B., Bronstein M., Kaufman J. R., Westrick R., Ginsburg D., 2007. Fatal hemorrhage in mice lacking γ-glutamyl carboxylase. Blood, 109: 5270-5275

Ziros G. P., Basdra K. E., Papavassiliou G. A., 2008. Runx2: of bone and stretch. The International Journal of Biochemistry and Cell Biology, 40: 1659-1663